UCSF
UC San Francisco Previously Published Works

Title

Prenatal AAV9-GFP administration in fetal lambs results in transduction of female germ cells and maternal exposure to virus.

Permalink

https://escholarship.org/uc/item/6dn0z2qh

Journal

Molecular Therapy: Methods & Clinical Development, 32(2)

ISSN

2329-0501

Authors

Borges, Beltran
Varthaliti, Antonia
Schwab, Marisa
et al.

Publication Date

2024-06-13

DOI

10.1016/j.omtm.2024.101263

Peer reviewed

eScholarship.org Powered by the California Digital Library
University of California

Molecular Therapy
Methods & Clinical Development
Original Article

Prenatal AAV9-GFP administration in fetal lambs results in transduction of female germ cells and maternal exposure to virus

Beltran Borges,[1,2,3] Antonia Varthaliti,[1,3] Marisa Schwab,[1,3] Maria T. Clarke,[1,2,3] Christopher Pivetti,[4] Nalin Gupta,[5,6] Cathryn R. Cadwell,[5,7,8] Ghiabe Guibinga,[9] Shirley Phillips,[9] Tony Del Rio,[9] Fatih Ozsolak,[9] Denise Imai-Leonard,[10] Lingling Kong,[11] Diana J. Laird,[3,12] Akos Herzeg,[1,2,3] Charlotte J. Sumner,[11,13,14] and Tippi C. MacKenzie[1,2,3,6,12]

[1]Department of Surgery, University of California, San Francisco, San Francisco, CA 94143, USA; [2]UCSF Center for Maternal-Fetal Precision Medicine, San Francisco, CA 94158, USA; [3]The Eli and Edythe Broad Center of Regeneration Medicine and Stem Cell Research, University of California, San Francisco, San Francisco, CA 94143, USA; [4]Department of Surgery, University of California, Davis, Davis, CA 95817, USA; [5]Department of Neurological Surgery, University of California, San Francisco, San Francisco, CA 94143, USA; [6]Department of Pediatrics and Benioff Children's Hospital, University of California, San Francisco, San Francisco, CA 94158, USA; [7]Department of Pathology, University of California, San Francisco, San Francisco, CA 94143, USA; [8]Weill Neurohub, University of California, San Francisco, San Francisco, CA 94158, USA; [9]Novartis Institutes for BioMedical Research Biologics Center, San Diego, CA 92121, USA; [10]Comparative Pathology Laboratory, University of California, Davis, Davis, CA 95616, USA; [11]Department of Neurology, Johns Hopkins University School of Medicine, Baltimore, MD 21218, USA; [12]Department of Obstetrics and Gynecology, University of California, San Francisco, San Francisco, CA 94158, USA; [13]Department of Neuroscience, Johns Hopkins University School of Medicine, Baltimore, MD 21218, USA; [14]Department of Genetic Medicine, Johns Hopkins University School of Medicine, Baltimore, MD 21218, USA

Prenatal somatic cell gene therapy (PSCGT) could potentially treat severe, early-onset genetic disorders such as spinal muscular atrophy (SMA) or muscular dystrophy. Given the approval of adeno-associated virus serotype 9 (AAV9) vectors in infants with SMA by the U.S. Food and Drug Administration, we tested the safety and biodistribution of AAV9-GFP (clinical-grade and dose) in fetal lambs to understand safety and efficacy after umbilical vein or intracranial injection on embryonic day 75 (E75) . Umbilical vein injection led to widespread biodistribution of vector genomes in all examined lamb tissues and in maternal uteruses at harvest (E96 or E140; term = E150). There was robust GFP expression in brain, spinal cord, dorsal root ganglia (DRGs), without DRG toxicity and excellent transduction of diaphragm and quadriceps muscles. However, we found evidence of systemic toxicity (fetal growth restriction) and maternal exposure to the viral vector (transient elevation of total bilirubin and a trend toward elevation in anti-AAV9 antibodies). There were no antibodies against GFP in ewes or lambs. Analysis of fetal gonads demonstrated GFP expression in female (but not male) germ cells, with low levels of integration-specific reads, without integration in select proto-oncogenes. These results suggest potential therapeutic benefit of AAV9 PSCGT for neuromuscular disorders, but warrant caution for exposure of female germ cells.

INTRODUCTION

Prenatal somatic cell gene therapy (PSCGT) could address numerous single-gene disorders such as spinal muscular atrophy (SMA) or muscular dystrophies before the onset of permanent organ damage.[1–3] Fetal therapy has several advantages over postnatal treatment, such as the possibility of targeting neurons prior to the maturation of the blood-brain barrier (BBB),[4] the potential for developing immune tolerance,[5,6] and the abundance of proliferating stem cells for gene targeting.[7]

The promise of a single definitive therapy given prior to the onset of organ damage is compelling. PSCGT is becoming increasingly feasible due to the expansion of other prenatal medical therapies (e.g., *in utero* enzyme replacement therapies for lysosomal storage disorders[8]) and improvements in prenatal diagnostics. The most severe forms of SMA are a particularly attractive target for fetal therapy, since carrier screening is recommended for all pregnant women,[9] disease pathology begins prior to birth, and neurodegeneration is most rapid in the neonatal period.[10] Moreover, neonates with severe SMA exhibit elevated plasma levels of the disease biomarker (phosphorylated neurofilament heavy chain) compared with age-matched controls, further indicating prenatal onset of pathology.[11]

Adeno-associated virus (AAV) vectors such as AAV serotype 9 (AAV9) are currently used in several clinical settings. Some of the advantages of AAV9 include the potential to cross the BBB[11] and transduce motor neurons,[12,13] low immunogenicity,[14]

Received 30 January 2024; accepted 1 May 2024;
https://doi.org/10.1016/j.omtm.2024.101263.

Correspondence: Tippi C. MacKenzie, MD UCSF School of Medicine Regeneration Medicine, Building 35 Medical Center Way RMB 900E, Campus Box 0665, San Francisco, CA, USA.
E-mail: tippi.mackenzie@ucsf.edu

This is an open access article under the CC BY-NC-ND license (http://creativecommons.org/licenses/by-nc-nd/4.0/).

a predominantly non-integrating profile,[15–17] and a notable tropism for neural tissue and striated muscle.[18] Onasemnogene abeparvovec-xioi (AVXS-101, Zolgensma) utilizes an AAV9 vector to deliver a replacement SMN cDNA and is approved for one time, intravenous (i.v.) delivery in infants with SMA less than 2 years of age.[19] Another AAV9 vector was recently approved for i.v. delivery in children with Duchenne muscular dystrophy (DMD) aged 4–8 years,[20] and AAV vectors are also being studied for intrathecal delivery to treat giant axonal neuropathy (NCT02362438).

AAV vectors have been tested in numerous models of prenatal gene therapy given their safety profile and likelihood of clinical translation. These experiments demonstrated tolerance to transgene-encoded proteins such as coagulation factors in mice[21,22] and non-human primates.[5,6] Disease correction was seen in mouse models of SMA,[23] hemophilia,[21,22] and neuronopathic Gaucher.[24] AAVs have also been used as a delivery vector for genome editors in fetal mouse experiments.[25,26] However, a thorough examination of maternal and fetal toxicity with a clinical-grade vector to assess barriers to clinical translation has not been performed.

Large animal experiments are important for pharmaceutical drug development, as they explore the pharmacokinetics, biodistribution, and toxicity of the studied agent.[27] In our study, we chose the fetal lamb model given the extensive experience for developing fetal surgery protocols, the similar size and physiology to human fetuses, and the low incidence of preterm delivery.[28,29] We tested a clinical-grade AAV9-GFP, a vector comparable with AVXS-101, but with a GFP transgene instead of SMN, at the same weight-based dose. We chose to do an open injection technique to avoid any technical variability from ultrasound-guided injections (which are performed routinely in humans, but are not readily translatable to this fetal lamb model, which has multiple fetuses and a different placental architecture). Our findings support previous reports[12,30,31] of broad biodistribution of AAV vectors across the neuraxis and in other tissues, but raise important safety considerations, particularly due to the observation of maternal exposure and germline transduction in female fetuses. Although viral integration is low, these findings may be particularly concerning if AAV vectors are used to deliver genome editors.

RESULTS

Experimental design and survival

The experimental design is depicted in Figure 1A. We included 30 fetuses from 15 pregnancies (Table S1). Thirteen fetuses were injected with a single dose of AAV9-GFP (2×10^{13} vg per fetus, equivalent to 1×10^{14} vg/kg, similar to the postnatal dose of onasemnogene abeparvovec-xioi) through the umbilical vein. Lambs were harvested at two time periods before birth, to enable readout of short-term events related to vector exposure in fetuses and dams: six lambs were harvested at E96 (3 weeks after injection) and seven were harvested at E140 (9 weeks after injection) (term = E150). Four additional fetuses were injected intracranially (IC) through the cisterna magna to access the subarachnoid space as a pilot to assess the feasibility of this approach (E96 harvest [n = 2]; E140 harvest [n = 2]). Figure 1B demonstrates the operative approach for these injections. Thirteen fetuses served as uninjected controls (E96 [n = 7]; E140 [n = 6]).

The overall fetal survival rate to harvest was 100% for the IC-injected fetuses, 84.6% for the umbilical vein group, and 92.3% for the non-injected controls (Figure 1C). There was no preterm labor seen. Three fetuses were found deceased at the time of harvest in two separate pregnancies: In one triplet pregnancy harvested at E96 (1966), we observed the demise of one umbilical vein-injected fetus and one uninjected control in the same uterine horn, while a third fetus (umbilical vein injected) in the other uterine horn survived (Figure S1A). Histological examination revealed acute suppurative placentitis (Figure S1B), with extensive necrosis in the placenta in both fetuses, suggesting an infectious etiology for the demise. A second twin pregnancy with umbilical vein injection of both fetuses (2134) demonstrated demise of one fetus at E140, while the second fetus in the other uterine horn was alive (Figure S1C). The histological examination of the demised fetus was limited by severe tissue friability, while the live littermate demonstrated neutrophilic chorioamnionitis with neutrophilic vasculitis, acute severe necrotizing placentitis with intralesional fungal hyphae, and mild extensive neutrophilic and lymphoplasmacytic endometritis (Figure S1D), again suggesting an infectious cause for fetal demise in this pregnancy.

We detected lower fetal harvest weights in the umbilical vein-injected animals harvested at E96 compared with uninjected controls, even when considering natural variation for lower weights of pregnancies with higher numbers of fetuses (Figure 1D). We observed a similar trend at E140 (Figure 1E) (e.g., in one quadruplet pregnancy with two injected fetuses, the injected fetuses were smaller than their uninjected littermates).

Vector biodistribution in CNS tissues of fetal lambs

We detected widespread vector biodistribution in the brains and spinal cords of fetal lambs at both time points and with both umbilical vein and IC injections (Figure 2). In umbilical vein-injected lambs, we detected higher levels of vector genomes at E96 compared with E140 (Figure 2A). We also confirmed widespread GFP expression by droplet digital PCR (ddPCR) for GFP mRNA in many CNS tissues examined from both IC- and umbilical vein-injected fetuses (Figure 2B). GFP staining confirmed the intense expression of the transgene in anterior horn neurons on all levels of the spinal cord (Figure 2C) at both time points.

We also examined dorsal root ganglia (DRGs) for GFP expression and cellular architecture. We detected robust GFP staining in DRG neurons at multiple levels in both umbilical vein- and IC-injected fetuses (Figure 2D, L5 DRG shown). Given the previously reported DRG toxicities observed with AAV9 vectors,[32–35] we also examined the cellular

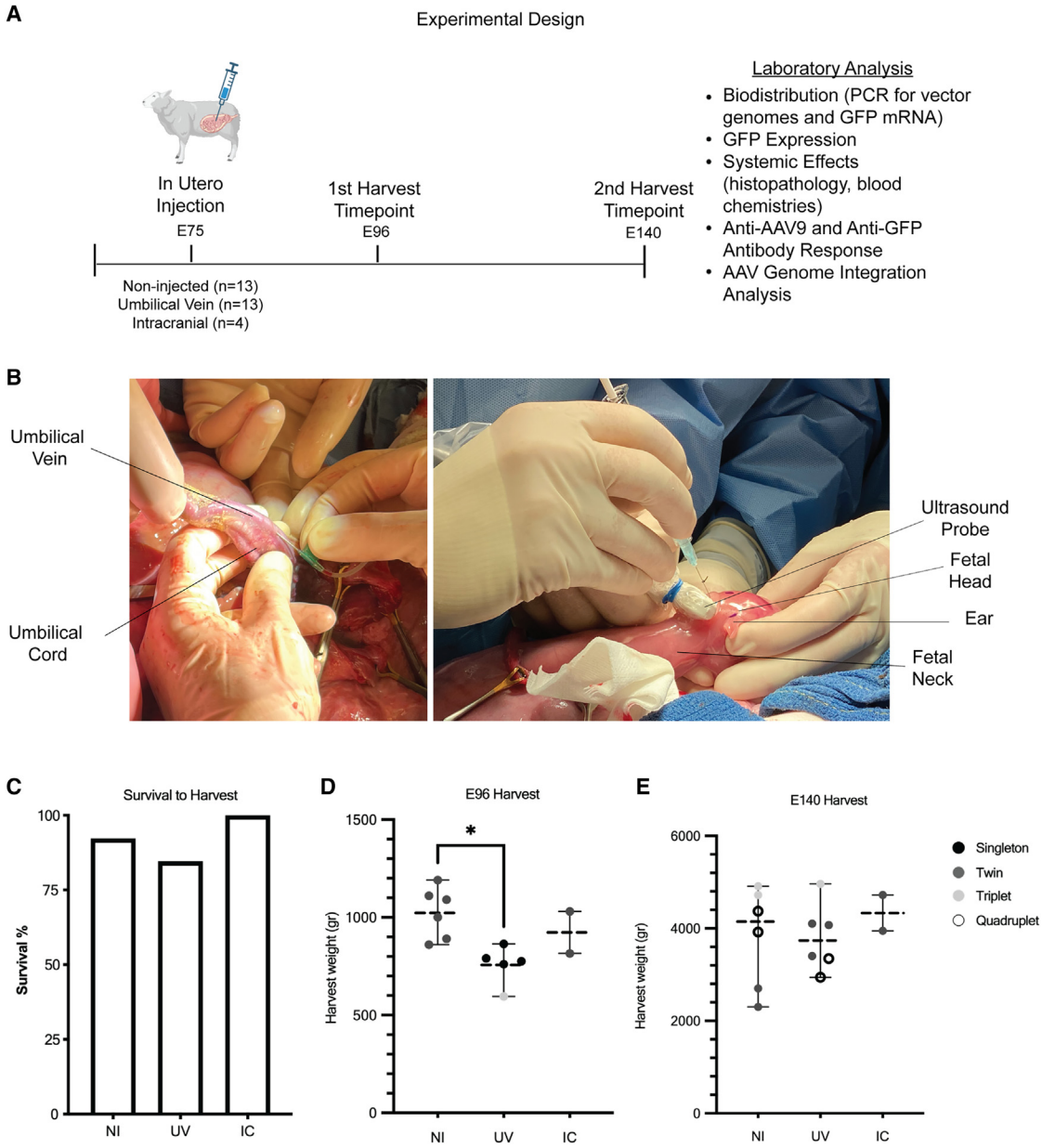

Figure 1. Experimental design and survival after *in utero* injection of scAAV9-GFP in fetal lambs

(A) Experimental design. Fetal lambs were injected on E75 with 1×10^{14} vector genomes/kg of sc-AAV9-GFP and harvested at E96 ± 1 day or E140 ± 3 days (term = E150). Image created with www.biorender.com. (B) Representative pictures of an umbilical vein injection (left) or an ultrasound-guided IC injection (right). (C) Survival to harvest (non-injected [NI, n = 13]; umbilical vein [UV, n = 13]; IC [n = 4]). (D and E). Harvest weights at E96 (D) or at E140 (E) based on litter size and experimental group. Each dot represents one fetus; symbols indicate total number of fetuses in each litter. Center lines and whiskers indicate mean and SEM, respectively. *$p < 0.05$ by one-way ANOVA with Tukey's multiple comparison test (n = 6 for NI and n = 5 for umbilical vein at E96). No significant differences were seen between groups at the E140 time point by one-way ANOVA with Tukey's multiple comparison test.

architecture of the DRGs for chromatolysis, axonal loss, axonal degeneration, and regenerating clusters. Although this analysis was partially limited by crush and traction artifacts, we did not detect any differences between uninjected controls and injected animals (Figures S2A and S2B). Ventral root axons were also examined with no pathological findings. Notably, the size and myelination of the axons is comparable with that in prenatal humans (Figure S2C), suggesting that the fetal lamb shows promise as a preclinical model for ventral root axons (as was also recently described for the fetal pig model[36]).

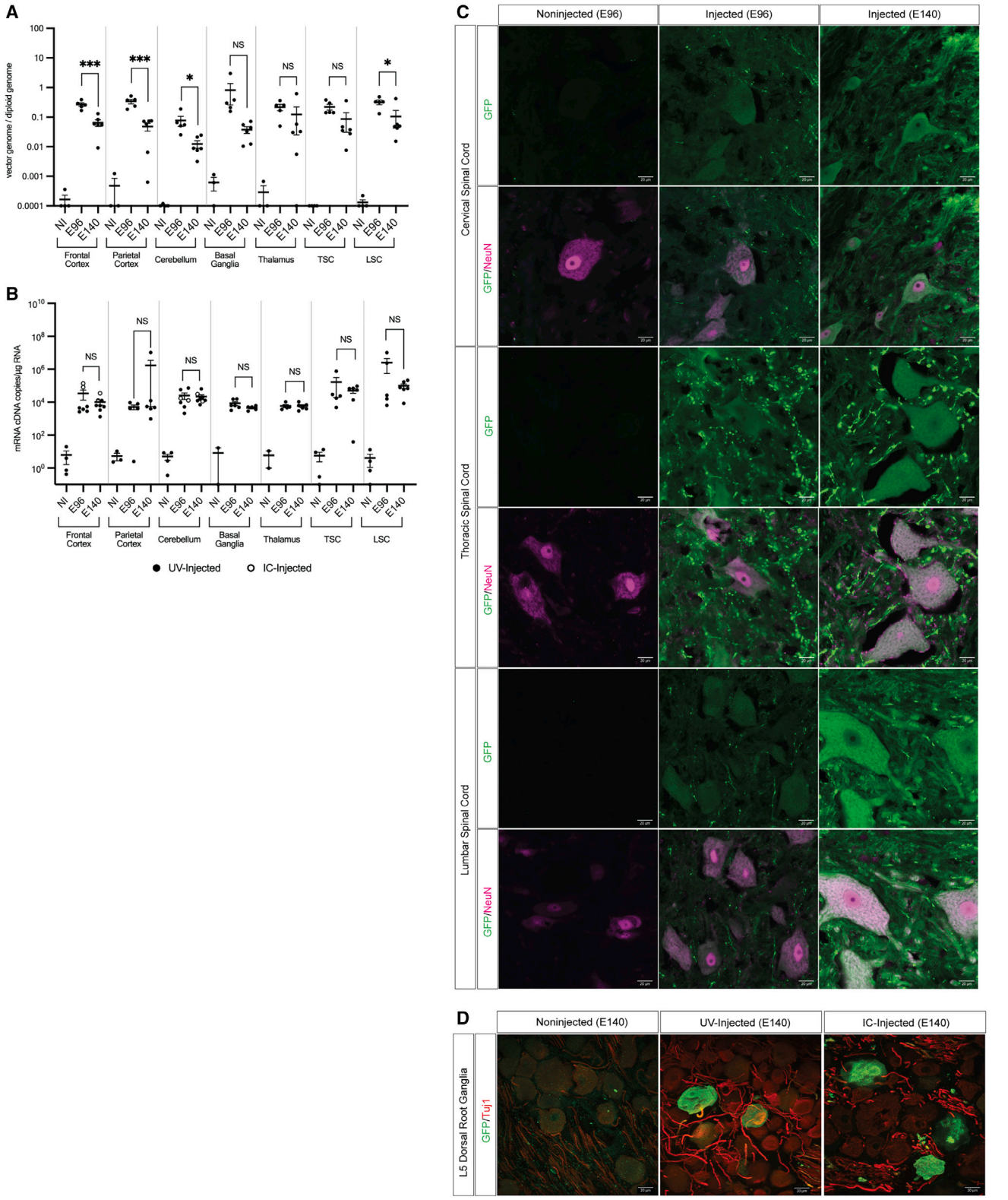

(legend on next page)

Vector biodistribution in non-CNS tissues of fetal lambs

In addition to multiple regions of the brain and spinal cord, we detected vector genomes in multiple peripheral tissues, including liver, spleen, heart, diaphragm, lung, thymus, and gonads. Similar to the findings in the CNS, we detected higher levels of vector genomes at E96 compared with E140 in multiple tissues (Figure 3A). We detected both vector sequences and GFP mRNA in the thymus, albeit at lower levels than other tissues by E140. Importantly, we detected vector sequences in both female and male gonad samples. We also confirmed GFP expression by ddPCR for GFP mRNA in all tissues examined from umbilical vein-injected fetuses (Figure 3B) with no apparent differences between harvest time points. Interestingly, there was systemic expression of GFP even after IC injection.

Consistent with the vector biodistribution data, we found widespread GFP expression with immunofluorescence in numerous tissues, particularly the quadriceps, diaphragm, and myocardium (Figure 3C). Quantification of GFP^+ myocytes in quadriceps demonstrated transduction rates at or above 75% of muscle cells in examined animals (Figure 3D). We also examined staining in the liver to identify whether AAV9 transduced hepatocytes and/or hematopoietic cells at this point in gestation. We found transduction of HNF-$4\alpha^+$ hepatocytes at both time points (Figure 3E). However, while $CD45^+$ leukocytes or $CD34^+$ hematopoietic stem cells were identified in the fetal liver at E96, these cells did not express GFP (Figure 3E).

Given the detection of vector genomes in female and male gonads (Figure 3A), we stained these tissues for GFP and the germ cell marker DDX4 (Figure 4).[37] We detected numerous GFP^+ cells in the male testes that did not stain with DDX4 and were located outside of the testis cords, indicating male germ cells were not transduced (Figure 4A). However, in the female ovaries, we detected numerous GFP^+ $DDX4^+$ cells, indicating transduction of female germ cells (Figure 4B).

Vector biodistribution in maternal ewes and in placentas

We evaluated the biodistribution of the vector in maternal tissues (liver, uterus, ovaries, and blood) and in the placentas (Figure S3A). We found that all examined maternal liver and ovarian samples had low vector genome levels, comparable with those of uninjected fetuses. Uterine samples (which also contain a layer of fetal membrane tissue from the harvest) had comparatively higher vector genome levels ($p = 0.05$ at E140 when compared with uninjected controls). Levels in the placenta were comparable with those observed in other fetal organs. Importantly, we did not find vector sequences in the blood of the ewes at either time point after injection (Figure S3B).

We also assessed maternal tissues for GFP mRNA expression (Figure S3C) and found that the levels in these tissues were not different from those of non-injected controls. Notably, of the livers examined, there was one outlier which corresponded with ewe 1966, potentially representing the effects of resorption of the demised fetal tissues.

Antibody responses

One potential benefit of *in utero* therapy is the induction of tolerance to transgene-encoded proteins and the lack of antibody formation to viral capsid antigens when the initial exposure is during the time of fetal immune development, as previously demonstrated after *in utero* injection in fetal monkeys.[5,6] We, therefore, analyzed antibodies against AAV9 capsid antigens, as well as against GFP (Figure 5). When we compared the maternal titers of IgM or IgG antibodies against AAV9 capsid antigens prior to dosing and at the time of harvest, we did not detect any increases in IgM levels at any time point (Figure 5A). There was a trend for higher levels of maternal IgG antibodies at E140 compared with pre-dose (Figure 5B). When we analyzed anti-AAV9 titers in the fetal lambs, we detected higher levels of IgM antibodies at the E96 time point (Figure 5C) compared with E140, consistent with the time frame of an IgM antibody response.[38] We also detected anti-AAV9 IgG antibodies after both umbilical vein and IC injections (Figure 5D), indicating an ability to mount an immune response by the fetal lamb at this gestational age, even after IC injection. Anti-AAV9 IgG antibody titers were higher at the E140 time point compared with E96, consistent with the predicted time frame for IgG antibody formation.[38] To understand whether the anti-AAV9 IgG antibodies seen in the fetuses could be maternal antibodies that have crossed the placenta, we evaluated ewe/lamb pairs together (Figure 5E) and detected higher titers of IgG antibodies in several lambs compared with their mothers, suggesting this may be a primary fetal immune response. Importantly, we did not detect any antibodies (IgG or IgM) against GFP protein in any of the injected lambs or in ewes (Figure 5F), indicating that long-term exposure to the transgene-encoded protein did not result in an immune response in the fetuses.

Systemic effects of prenatal exposure to AAV9-GFP

To understand whether exposure to AAV9-GFP resulted in systemic toxicities, we measured liver function tests and blood chemistries in ewes, comparing levels before injection with those obtained at

Figure 2. Biodistribution of scAAV9-GFP in the CNS after prenatal administration

(A) Vector genome copies per diploid genome (vg/dg) in various CNS tissues after prenatal umbilical vein injection and harvest at E96 or E140. Each dot represents one fetus. Center lines and whiskers indicate mean and SEM, respectively. *$p < 0.05$ and **$p < 0.01$ by parametric, unpaired, two-tailed t tests ($n = 5$ for E96 and $n = 6$ for E140). LSC, lumbar spinal cord; TSC, thoracic spinal cord. (B) GFP mRNA copies/μg RNA in various CNS tissues of umbilical vein-injected (filled circles) and IC-injected (open circles) fetuses harvested at E96 and E140. Each dot represents one fetus. Center lines and whiskers indicate mean and SEM, respectively. No significant differences were seen between time points by parametric, unpaired, two-tailed t tests. (C) Representative images of GFP expression (green) and NeuN (pink) in cervical (top row), thoracic (middle row), and lumbar spinal cord (bottom row) in the indicated experimental groups (original magnification ×63). (D) Representative images of GFP expression (green) and Tuj1 (red) in lumbar DRG in indicated experimental groups (original magnification ×63). NI, non-injected; UV, umbilical vein.

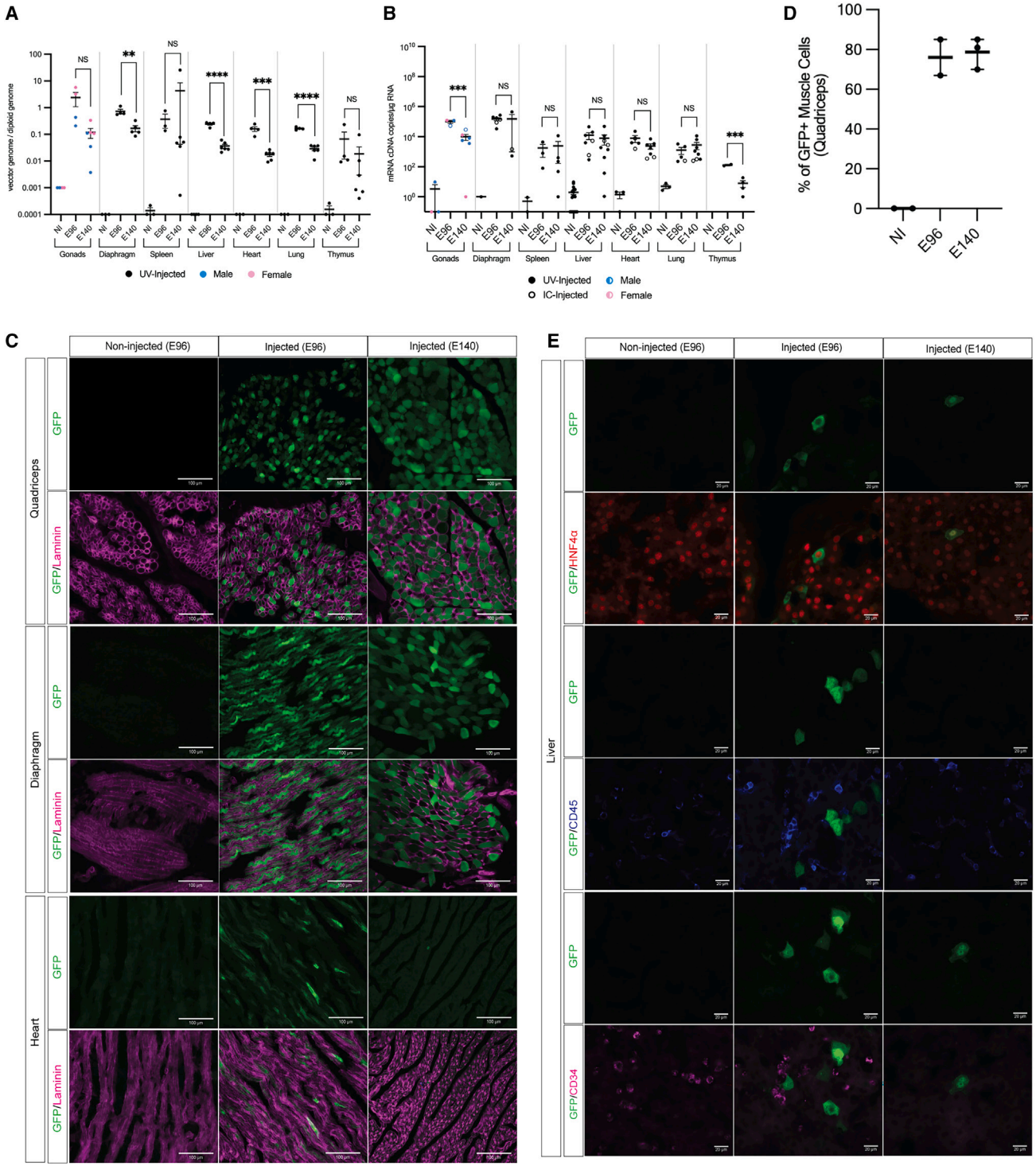

Figure 3. Biodistribution of scAAV9-GFP in peripheral tissues after prenatal administration

(A) Vector genome copies per diploid genome (vg/dg) in various peripheral tissues after umbilical vein injection and harvest at E96 or E140. Each dot represents one fetus. Blue dots represent male fetuses; pink dots represent female fetuses. Center lines and whiskers indicate mean and SEM, respectively. *$p < 0.05$, **$p < 0.01$, and ****$p < 0.0001$ by parametric, unpaired, two-tailed t tests ($n = 4$ for E96 and $n = 6$ for E140). (B) GFP mRNA copies/µg RNA in various peripheral tissues of umbilical vein-injected (filled circles) and IC-injected (open circles) fetuses harvested at E96 and E140. Each dot represents one fetus. Blue dots represent male fetuses. Pink dots represent

(legend continued on next page)

multiple time points after injection up to the time of harvest. These chemistries were stable and largely within normal ranges (Figure 6A). However, we did detect an increase in total bilirubin in several ewes (one of which had a pregnancy with fetal demise). There was a statistically significant increase in maternal alkaline phosphatase and decreases in blood urea nitrogen (BUN) and creatinine, but levels remained in the normal range.

Similarly, liver and kidney function tests were examined at the time of harvest in all fetal lambs and were mostly within the ranges seen in uninjected controls; the only change seen with *in utero* exposure to AAV9 was an increase in the mean total bilirubin in the umbilical vein-injected group compared with uninjected controls at the E96 harvest time point (Figure 6B), which was not seen at E140.

We performed a full autopsy on all lambs at both time points. While most tissues did not demonstrate any pathological changes after *in utero* injection, we detected renal tubular epithelial necrosis and pigment accumulation at the E96 harvest time point in all injected lambs (Figure 6C). Hepatic pigment accumulation and bile canalicular stasis was present in treated fetuses, but also present in a subset of controls. To determine whether the degree of pathology was linked to *in utero* exposure to AAV, all kidney and liver tissues were scored for the degree of such changes by a pathologist blinded to the experimental group. There was an increase in the kidney pathology scores after *in utero* AAV9-GFP exposure at E96 (Figure 6D). Interestingly, these changes were seen in both umbilical vein- and IC-injected fetuses, suggesting systemic exposure after IC injection at this gestational age. However, these changes were not evident at the E140 harvest point, suggesting resolution of the insult. There were no differences in the liver scores between *in utero*-injected animals and uninjected controls at either time point (Figure 6E).

Vector integration analysis

Given the finding of vector sequences and GFP expression in gonads, we performed integration analysis in gonads of six umbilical vein-injected fetuses (three male and three female) harvested at E140 by doing standard shearing-extension primer tag selection ligation-mediated PCR (S-EPTS/LM-PCR) (Figure 7A). Each sample was split into three technical replicates, and among an average of 130,274 ± 7722 (SEM) sorted reads/replicate, we detected an average of 61 ± 20 (SEM) integration-specific reads/replicate (Figure 7B). Mapping these integration-specific reads to the sheep genome yielded 2.22 ± 0.3 (SEM) integration sites (ISs) per sample. Importantly, none of the ISs were conserved among technical replicates, suggesting low risk of clonal expansion after genomic integration. ISs were distributed among most sheep chromosomes (Figure 7C) and were found both upstream and downstream of the coding regions (Figure 7D).

Figures S4A–S4F further demonstrate the relative distribution of ISs for each sample. An in-depth analysis of the genes that had ISs denotes a diverse profile of functions including neurotransmitter receptors (GRID2, GABRG3, and GABRB3), gene expression regulation (MBTD1, MYOCD, DACH1, CAMTA1, and E2F2), cell division and differentiation regulation (CREG1, VGLL4, and NCAPH2), and neuronal morphogenesis (ARHGEF28), among others (Table S2).

To understand the risk of insertion into cancer-associated genes, we extrapolated ISs from their sheep genomic positions to the human genome (possible in 21/40 sequences). None of the ISs were located within, or close to, proto-oncogenes that have been implicated in adverse events such as clonal outgrowth, leukemia, or myelodysplastic syndrome in clinical gene therapy studies using retroviruses (e.g., CCND2, HMGA2, LMO2, MECOM, and MN1).[39–44] Four of the ISs were within a window of 100 kB from transcription start sites of certain cancer-associated genes (TPM3, MDS2, ID3, and CD79B).

DISCUSSION

The primary aim of this study was to evaluate the safety and efficacy of a systemic injection of an AAV9-GFP vector (similar to the one used clinically to treat patients with SMA and at the same dose) in a fetal lamb model to determine the risks and benefits of a potential of a clinical application in fetuses with severe SMA. Consistent with the expected biodistribution of AAV vectors in the fetal environment, we detected robust transgene expression in the CNS and peripheral tissues. Notably, efficient transduction of muscle and diaphragm and a lack of antibody formation against the transgene-encoded protein are also encouraging for applications of AAV9 gene therapy in conditions such as muscular dystrophy. However, we noted several findings that require further consideration, including maternal exposure to the vector, apparent fetal growth restriction, transient increases in total bilirubin, and transient changes in kidney pathology. We also detected transduction of female, but not male, germ cells in the fetus, with a low level of genomic integration events. Our results highlight the need for more studies to determine the extent to which some of these findings could be ameliorated by dose titration and/or a less invasive injection technique. These results also warrant further multidisciplinary discussions for considering prenatal use of AAV vectors that are currently approved by the U.S. Food and Drug Administration (FDA) for the treatment of children with severe, early-onset genetic conditions and, critically, invite caution for the prenatal use of AAV vectors to deliver genome editors.

female fetuses. Center lines and whiskers indicate mean and SEM, respectively. No significant differences were seen between time points by parametric, unpaired, two-tailed t tests. (C) Representative images of GFP expression in quadriceps (top row), diaphragm (middle row), and heart (bottom row) after umbilical vein injection and harvest at the indicated time points (original magnification ×20). Pink, laminin. (D) Quantification of GFP^+ myocytes in quadriceps after prenatal umbilical vein injection. Each dot represents one fetus. Center lines and whiskers indicate mean and range, respectively. No significant differences were seen between time points by Mann-Whitney test. (E) Representative images of GFP expression in various cell types in fetal liver after umbilical vein injection. Hepatocytes (HNF-4α, top); leukocytes (CD45, middle), and hematopoietic stem cells (CD34, bottom) (original magnification ×63). NI, non-injected; UV, umbilical vein.

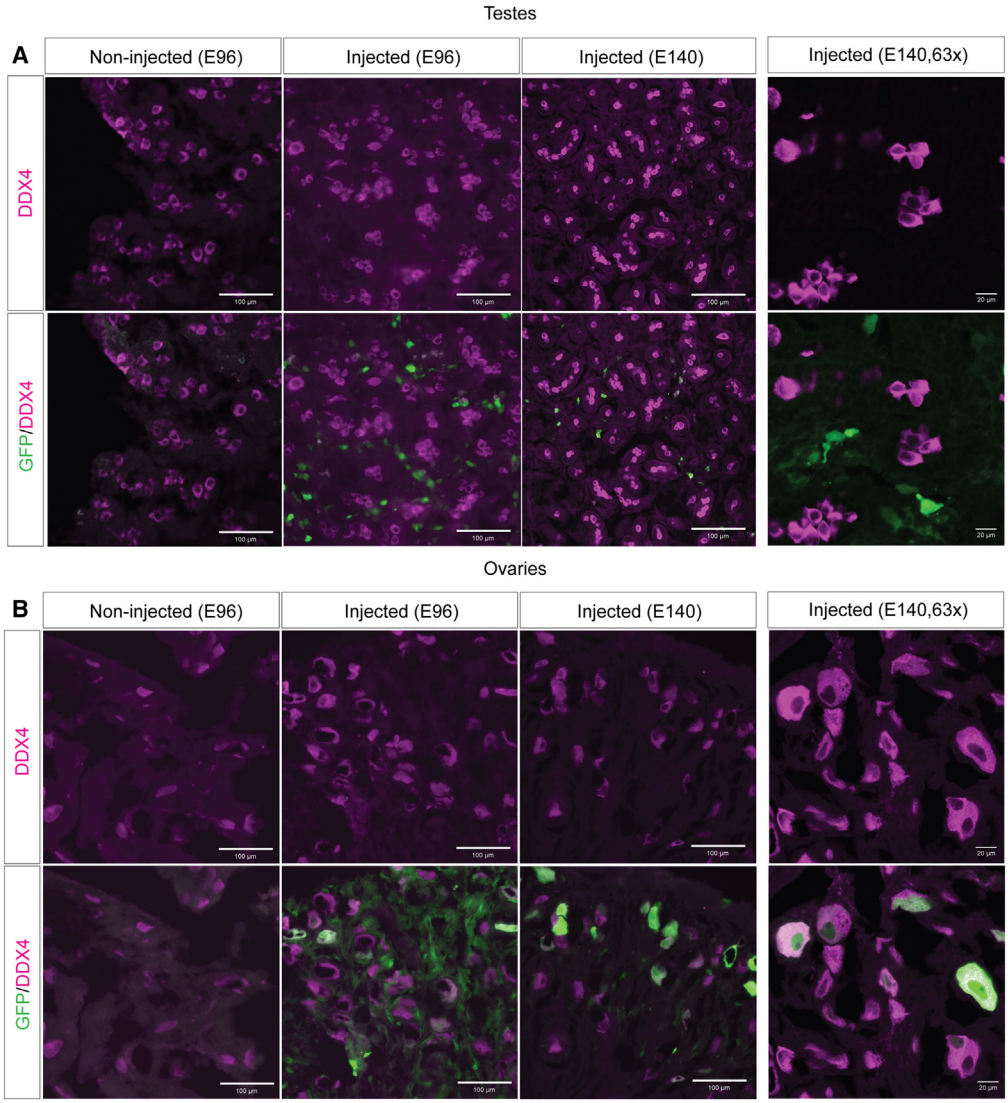

Figure 4. Detection of scAAV9-GFP in fetal gonads after prenatal administration

Representative images of GFP expression by cells in gonads after prenatal umbilical vein injection in testes (A) or ovaries (B) of fetal lambs at the indicated time points (original magnification ×20; last column, original magnification ×63). Co-localization of GFP with the germ cell marker DDx4 (pink) was not seen in testes, but was detected in ovaries.

AAV gene therapy has many advantages as evidenced by several approaches that are now FDA-approved, including those for SMA,[19] DMD,[20] and hemophilia.[45] However, this approach (particularly at high doses) also carries the risk of various toxicities in both human and animal studies, including thrombotic microangiopathy,[46] DRG sensory neuron degeneration,[32–35] and liver damage ranging from mild transaminase elevation and liver inflammation to patient death secondary to fulminant hepatitis.[32,47–50] Of note, in human trials, many patients have required corticosteroids to dampen AAV-mediated hepatotoxicity.[47–50] In this study, we did not need to administer prophylactic steroids and the only organ-specific changes we observed were transient elevations in fetal bilirubin and kidney lesions on histology (with normal BUN and creatinine), which resolved spontaneously by E140. Importantly, we did not observe DRG toxicity, even with direct injection of high-dose vector into the cisterna magna. While DRG toxicity has not been evaluated previously with prenatal large animal studies of AAV, our results align with a recent meta-analysis that showed that earlier (postnatal) ages at injection are correlated with decreased pathology scores on non-human primate DRGs.[33] Thus, there are important potential advantages of prenatal gene therapy with AAV vectors compared with postnatal use.

However, we detected some toxicities that have not previously been reported in a large animal model, including an apparent growth restriction after umbilical vein injection. In our study, we chose to

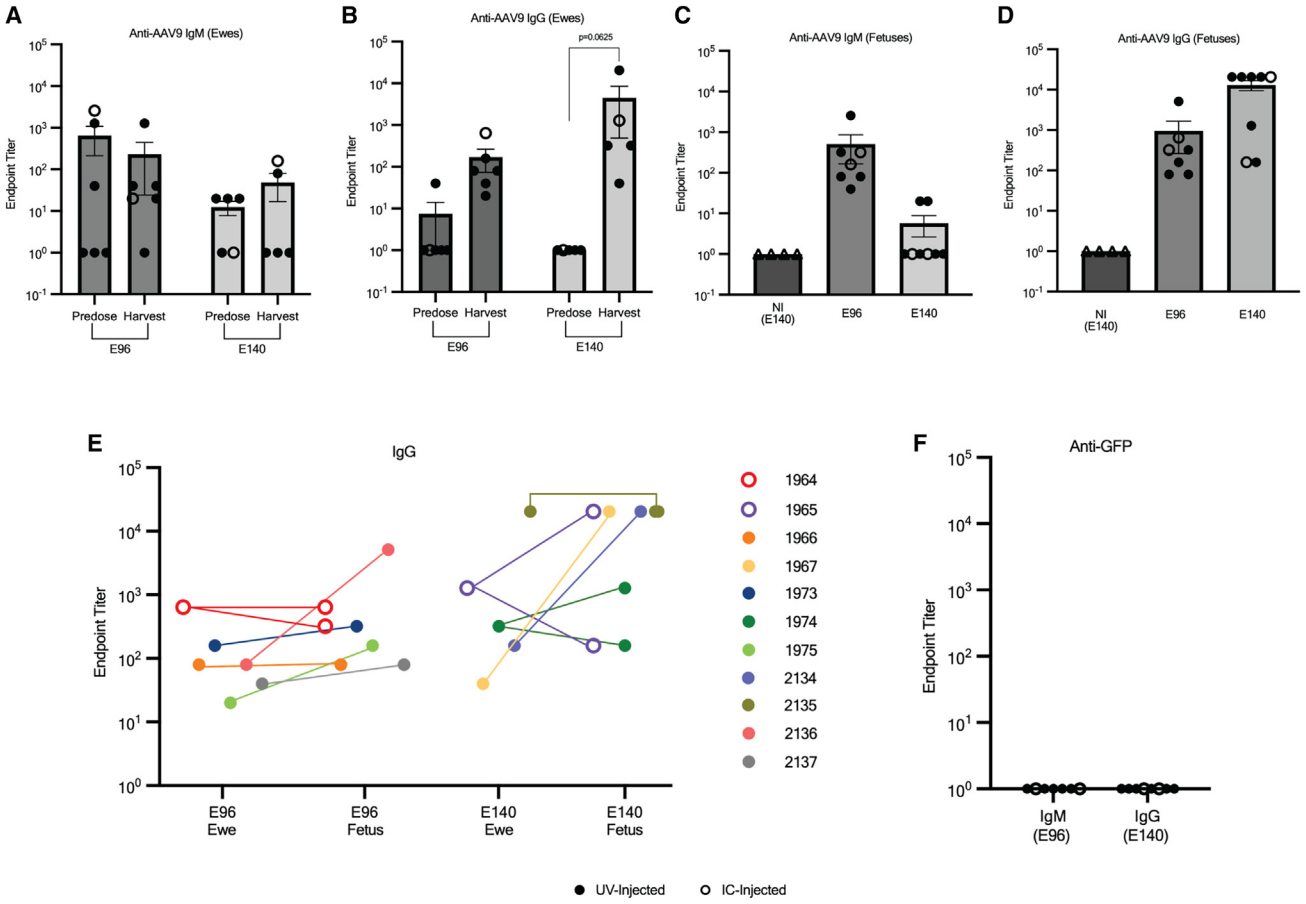

Figure 5. Detection of Anti-AAV9 IgM and IgG antibodies in maternal ewes and lambs after prenatal exposure to scAAV9-GFP

(A and B) Anti-AAV9 IgM (A) and IgG (B) endpoint titers prior to prenatal injections (predose) and at the time of harvest in ewes whose fetuses underwent umbilical vein injection (filled circles) or IC injection (open circles) of scAAV9-GFP. Each dot represents one ewe. Center lines and whiskers indicate mean and SEM, respectively. (C and D) Anti-AAV9 IgM (C) or IgG (D) endpoint titers at the time of harvest in non-injected fetuses (open triangles) and fetuses that underwent umbilical vein injection (filled circles) and IC injection (open circles). Each dot represents one fetus. Center lines and whiskers indicate mean and SEM, respectively. $p > 0.05$ between time points by Wilcoxon signed rank test in both IgG and IgM of fetuses and ewes. (E) Paired maternal-fetal anti-AAV9 IgG endpoint titers at the time of harvest after umbilical vein injection (filled circles) or IC injection (open circles) of scAAV9-GFP. (F) Anti-GFP IgM and IgG endpoint titers at the specified times of harvest in fetuses who underwent umbilical vein injection (filled circles) and IC injection (open circles). E96 = 3 weeks after injection; E140 = 9 weeks after injection.

use a dose equivalent to the clinical dose of AVXS-101, similar to our strategy for *in utero* enzyme replacement therapy,[8] for which we obtained FDA approval to infuse a fetal enzyme dose that is equal to the weight-adjusted clinical dose for neonates. Notably, our study dose (umbilical vein injections) was approximately 2 times,[5] 7 times,[5,6,51] and 70 times[52] higher than those used in previous large animal studies of prenatal AAV gene therapy that did not report fetal growth restriction, so it is possible that dose titration could mitigate this toxicity. In normal sheep pregnancies, there are several factors influencing fetal weight,[53,54] and we analyzed the data according to confounders such as litter size and sex of the lamb to account for such differences. It is also possible that some of the observed toxicities are not due to the AAV itself, but rather a result of gestational age discrepancies, fetal manipulation, transient umbilical cord spasm after injection, and/or transgene expression (the latter has been reported for both GFP[55] and SMN[32]). Importantly, the cases of fetal demise in this study were related to infection and do not seem to be a result of the AAV.

Maternal safety is the most important consideration for any fetal therapy effort. Our findings of anti-AAV9 IgG antibody development suggest some exposure of the mother to the vector after administration into the fetus. Potential sources of exposure to the vector could be through the maternal-fetal interface (based on our finding of higher levels in the uterus/fetal membranes compared with non-injected controls) or through the placenta. Of note, among the examined maternal liver tissues, only the ewe with two demised fetuses had high levels of GFP mRNA; it is possible that maternal exposure to viral transduction was increased with resorption of demised fetal tissues. Importantly, there are differences in placental structure

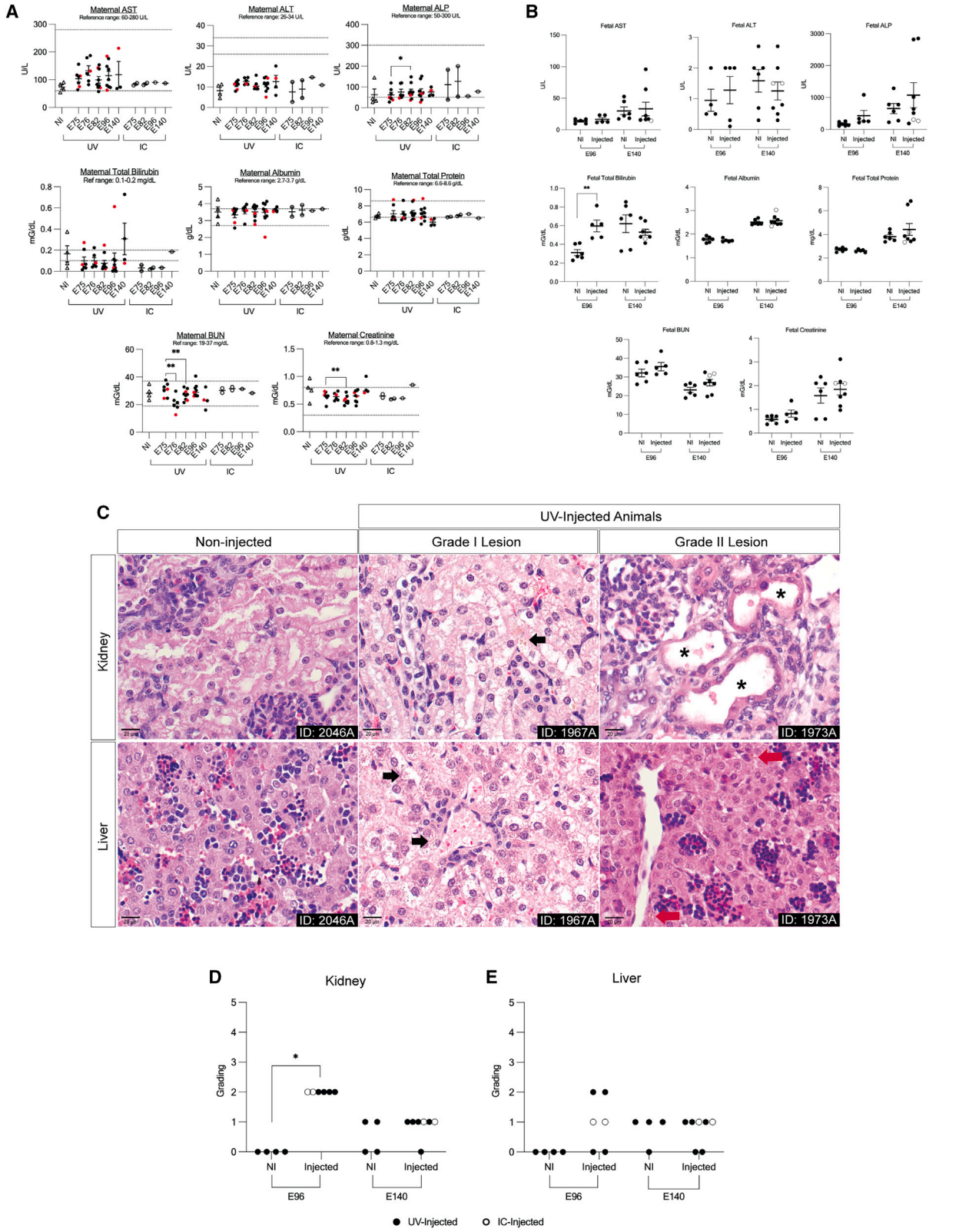

(legend on next page)

between humans and sheep,[56] and maternal exposure in humans could be different.

Immune responses to transgene-encoded proteins can also result in significant morbidities (as recently reported in patients with DMD receiving SRP-9001[57]), underscoring the importance of anticipating and preventing such immune responses in patients for whom the transgene-encoded protein is a completely novel antigen. In this context, our findings of lack of anti-GFP antibody response support previous reports of using the strategy of prenatal exposure to induce tolerance for conditions in which such immune responses limit therapeutic benefit. However, we note that prenatal administration does not tolerize to capsid antigens, likely since these antigens are transient while there is continued expression of GFP, including in the thymus. While our injection time point (E75) is likely after the pre-immune developmental period defined for *in utero* stem cell transplantation,[2] the anti-capsid antibody titers in our study are still lower than those reported with the same vector injected into adult female macaques[58] or those found in children with SMA who received onasemnogene abeparvovec-xioi (mean titers in the range of 10^5 in both instances[59]).

The most concerning finding in our study is the transduction of female germ cells. While the intent of prenatal gene therapy is the correction of somatic cells, this finding suggests that there may be an inadvertent transduction of germ cells in female fetuses. Interestingly, fetal male germ cells seem to not be affected. We hypothesize that the increased susceptibility of female germ cells is that oocytes are undergoing meiotic prophase during fetal development,[60] while male spermatogonia remain premeiotic until the later in life.[61] Our histological evaluation of germ cell transduction is consistent with (but more detailed than) a previous report of autopsy findings in infants who received onasemnogene abeparvovec-xioi,[30] which demonstrated the presence of AAV vector genomes in gonadal tissues, but the lack of histological analysis in this study prevents a direct comparison of the specific cell types that were transduced.

AAV vectors tend to remain episomal and would, therefore, not be passed to future generations, unless there is genomic integration in a transduced germ cell. Given previous reports of integration events with AAV injection,[5,6,25,62] we focused our analysis on gonadal tissues and found rare AAV integration events with a low risk of clonal expansion. While integration can result in the development of tumors in animal models,[63] we noted a random integration profile away from genes previously involved in severe adverse events in gene therapy trials.[39–44] Conversely, integration in somatic cells may have long-term therapeutic benefits, as it could potentially lead to sustained gene expression and the correction of disease in animal models of hemophilia[5,6,62] and Angelman syndrome.[25] Based on these excellent reports, we did not design our study to test the duration of GFP expression.

Even without integration, transduction of germ cells would result in germline editing if the AAV vectors were used to deliver a gene editor. One important ethical consideration for this scenario is the probability that such an event (occurring inadvertently in context of medical therapy for a fetus with a severe genetic condition) would result in a pregnancy in the next generation. Based on the number of oocytes in the female gonad at birth (600,000) compared with those that are ovulated over the course of reproductive years[64] (300, or 0.005%), and that only a fraction of these will result in a successful pregnancy, our data suggest that this is a small, albeit not zero, possibility. For the gene editing field, further improvements in the design of delivery vectors to either be non-functional in germ cells (such as by adding germ cell-specific microRNA target sequences at the 3′ end of the nuclease mRNA to limit gene expression[65]) or avoid transduction altogether are feasible strategies to decrease this risk even further. Another possibility is to focus on X-linked disorders for initial clinical applications. Therefore, our findings of robust transduction of skeletal muscle are particularly interesting given the promise of AAV vectors for muscular dystrophies (NCT03368742, NCT03362502).[20]

SMA remains a compelling target for prenatal therapy, as it is one of the most common inherited, infantile causes of death worldwide. The American College of Obstetrics and Gynecology currently recommends carrier screening for SMA in all pregnant women,[9] and improved screening strategies would likely yield even more prenatal diagnoses. Moreover, a recent survey conducted on the parents of children with SMA showed that most parents would be willing to enroll in a clinical trial testing of a prenatal gene therapy approach.[66] Given that irreversible motor neuron damage[10] and elevated neurofilament levels[11] are already present at birth in patients with SMA type 1, and that even patients treated postnatally before symptom onset can have motor function scores below normal and limited milestone achievement,[67] we think this disease would be amenable for prenatal therapy. The findings of transduction throughout the spinal cord and the lack of DRG toxicity are

Figure 6. Serum chemistries and relevant histology analysis in ewes and lambs after prenatal exposure to scAAV9-GFP

(A) Maternal ewe blood tests obtained serially at the indicated time points. Each circle represents one ewe; red circles denote ewes with a fetal demise. Lines represents the lower and upper limit of normal. Center lines and whiskers indicate mean and SEM, respectively. *$p < 0.05$ by parametric, paired, two-tailed t tests. (n = 7 for E75, n = 6 for E76 and n = 9 for E96 for ewes with umbilical vein-injected fetuses.) (B) Fetal lamb blood tests with and without *in utero* injection of scAAV9-GFP at indicated harvest time points. Open circles represent IC-injected fetuses. Each dot represents one fetus. Center lines and whiskers indicate mean and SEM, respectively. **$p < 0.01$ by parametric, unpaired, two-tailed t tests. (n = 6 for NI and n = 5 for injected at the E96 harvest.) (C) Representative hematoxylin and eosin images of grades I and II lesions in kidney (top row) and liver (bottom row) in the indicated groups (original magnification ×40). Kidney and liver grade I lesions show intracellular pigment accumulation (black arrows); kidney grade II lesions show tubular epithelial necrosis (asterisks); liver grade II lesions show bile canalicular stasis (red arrows). (D and E) Kidney (D) and liver (E) lesion scores for injected and uninjected fetuses at E96 and E140. Each dot represents one fetus. Open circles represent IC-injected fetuses. *$p < 0.05$ by nonparametric, Wilcoxon signed rank test (n = 4 for NI and n = 6 for injected at E96).

A

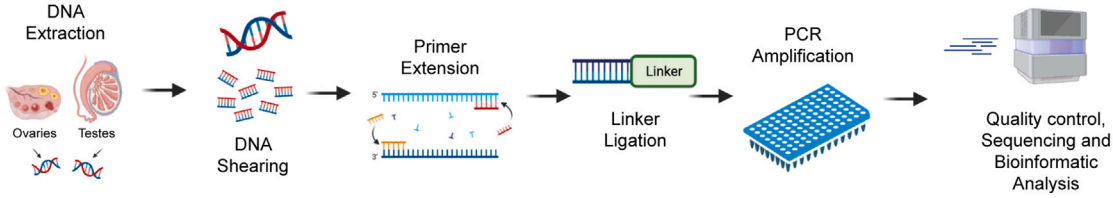

B

Lamb ID	Sex	Replicates	Sorted Reads	IS-Specific Reads	Integration Sites	Genes with Integration Sites
1967A *(vg/dg= 0.108)*	F	1967A-1	127754	55	3	FAM19A2, SLC7A11, LOC105605341
		1967A-2	122759	115	3	SPAG17, MBTD1, *ROCK2*
		1967A-3	137161	20	2	MGAT4C, LUZP2
1974B *(vg/dg= 0.117)*	F	1974B-1	88460	20	2	COL25A1, ARHGEF28
		1974B-2	109985	216	5	CREG1, GABRB3, MYOCD, LOC101107137, LOC101110483
		1974B-3	77691	10	1	DACH1
2134B *(vg/dg=0.337)*	F	2134B-1	106293	9	2	ANXA5, GPR26
		2134B-2	81880	92	1	CXCR1
		2134B-3	88039	0	0	-
2135A *(vg/dg=0.034)*	M	2135A-1	142469	26	1	UBAP2L
		2135A-2	164076	18	3	LOC105607638, NCAPH2, *ROCK2*
		2135A-3	176864	11	2	E2F2
2135B *(vg/dg=0.003)*	M	2135B-1	155000	316	3	PDCL3, IGSF22, LOC105612660
		2135B-2	166739	2	1	GPC5
		2135B-3	117325	0	0	-
1974C *(vg/dg=0.109)*	M	1974C-1	170142	70	3	C1H3ORF17, LOC101108158, GRID2
		1974C-2	153547	104	3	VGLL4, CAMTA1, LOC101108163
		1974C-3	158740	5	5	GH, GABRG3, LOC101120067, LOC105615237, DCAF12L2

C

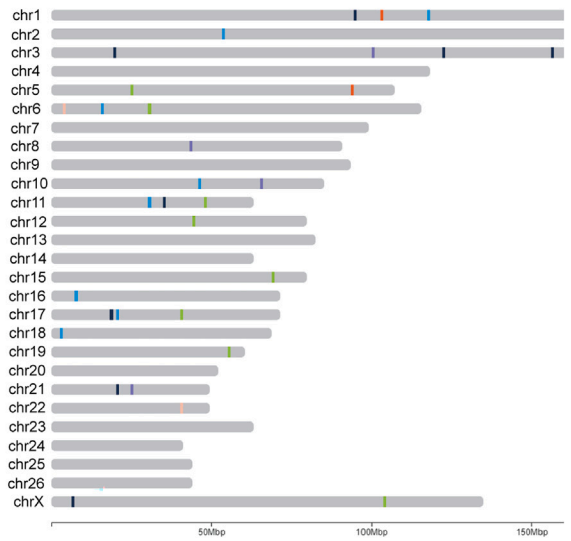

D

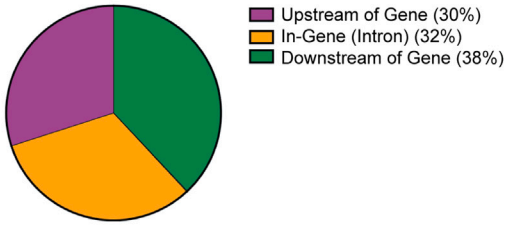

(legend on next page)

both encouraging for the efficacy and safety of this approach for the prenatal treatment of SMA.

We have performed a comprehensive analysis of outcomes after the *in utero* delivery of a clinical-grade vector in fetal lambs. Although our observations of widespread biodistribution into the CNS and lack of immune responses to GFP are encouraging, the finding of female germ cell transduction is sobering, particularly if AAVs were to be used to deliver genome editing machinery. We highlight the need for further studies and a balanced discussion of risks and benefits to ensure the development of safe and effective gene therapies for future patients.

MATERIALS AND METHODS

Vector

The vector used in the protocol for this project is AAV9-GFP (scAAV9-CB-GFP), provided by Novartis (Novartis AG, Basel, Switzerland). The manufacturing process for the vector used in this study was similar to that of the clinical-grade vector and based on guidelines for *in vivo* research use for the percentage of empty capsid and total purity, number of process-related impurities, plasmid DNA or production cells, endotoxin concentrations ($\leq$5.0 EU/mL). Each fetus (estimated weight of 200 g) was injected with 2×10^{13} vg (1.1×10^{14} vg/kg). Fetal weight was estimated based on previous reports.[68,69]

Surgical technique and prenatal injections

All animal handling complied with and was approved by the Institutional Animal Care and Use Committee of the University of California, San Francisco, and University of California, Davis. In this study, we chose to perform an open procedure with direct umbilical vein injection to ensure accurate delivery into the fetal circulation. After induction of general anesthesia and confirmation of pregnancy by ultrasound examination, a midline laparotomy was performed, followed by a hysterotomy of the uterine horn to expose the fetus. For the umbilical vein injection, a 27G butterfly needle was inserted into the umbilical vein in a free loop of cord, fetal blood was aspirated to confirm placement, and the vector (diluted in saline to a volume of 1.5 mL) was injected. For IC injections, sterile ultrasound (Wisonic Piloter Vet Ultrasound Diagnostic System) was used to visualize the cisterna magna in the sagittal plane. The junction between the occipital bone and the upper cervical spine was identified and marked on the skin. Under direct ultrasound visualization, a 25G needle was advanced through a midline entry point in the skin, usually with a slight rostral angulation so the subarachnoid space was reached by passing immediately inferior to the margin of the occipital bone. A total volume of 0.4 mL was injected. The uterus was closed after amniotic fluid replacement with saline and antibiotics (penicillin-gentamycin). The abdomen was closed in layers and the ewe was recovered per protocol. In some pregnancies, uninjected littermates served as controls, while in others, time-dated pregnancies without *in utero* manipulation served as pure controls.

Tissue harvesting

For both harvest time points (E96 and E140), the ewe was anesthetized and a laparotomy and hysterotomy were performed to deliver the fetus(es). After delivery, neonatal blood was drawn from the internal jugular vein, the lamb was euthanized with 100 mg/kg sodium pentobarbital (i.v.) and perfused with PBS. After extraction of the fetuses, maternal tissues were harvested, and ewe was euthanized with 0.5 mL/kg potassium chloride (i.v.).

ddPCR quantitation of vector genome copies

Tissues were processed for vector genome quantitation as previously described.[58] Briefly, sample tissues were collected, flash frozen in liquid nitrogen, and stored at −80°C until analyzed. For vector genome, collected tissues were analyzed using ddPCR quantitation with a C1000 Thermal Cycler (Bio-Rad, Hercules, CA, USA) and specific primers and probes. The assay allows the evaluation of the number of scAAV9-CB-GFP vector genomes, a two-copy reference gene (*RPP30*) was also quantified for normalization purposes. *RPP30* primers and probe were added in the master mix along with scAAV9-CB-GFP primers and probe. scAAV9-CB-GFP genomes and *RPP30* genes were quantified in the same reaction using multiplex ddPCR. The resulting values of scAAV9-CB-GFP were presented as vg/diploid genome, thus normalizing vector genomes to the *RPP30* reference gene. The limit of quantitation was 28 vector genome copies per 20-mL well. Of note, this is the same limit of quantitation determined for onasemnogene abeparvovec-xioi vector genome, since scAAV9-CB-GFP shares the same non-transgene components of the expression cassette. IC-injected animals are graphed, but the low numbers preclude statistical analysis of this group. Non-injected fetal values are obtained from both E96 and E140 harvest time points. For maternal tissues, non-injected values are obtained from all uninjected fetal tissues.

RNA extraction and ddPCR quantitation of AAV-9-GFP mRNA

Biodistribution of GFP mRNA transcript was also assessed in the collected tissues using RT-PCR as adapted from previously described.[70] In brief, total RNA was isolated using ZYMO kit or Promega maxwell system. RNA was reverse transcribed and quantified during the one-step ddPCR with multiplex primer and probes specific to GFP, with RNA concentration expressed as ng/mL. Non-injected fetal values are obtained from both E96 and E140 harvest time points. For maternal tissues, non-injected values are obtained from all uninjected fetal tissues.

ELISA detection of anti-AAV9-antibodies

The IgG and IgM antibody responses to the AAV9 capsid before and after vector dosing was assessed using binding ELISA as

Figure 7. Analysis of genomic integration of scAAV9-GFP in gonadal tissues

(A) Schematic outline of shearing extension primer tag selection ligation mediated PCR (S-EPTS/LM-PCR) to amplify AAV vector-genomic fusion sequences. Image created with www.biorender.com (B) Details of total sorted reads, IS-specific reads, ISs and genes with associated ISs in each replicate. (C) Distribution of AAV vector ISs in each chromosome (Chr); different color codes refer to unique samples as indicated in the legend. (D) IS location with respect to transcription sites.

previously described,[31] but adapted for sheep plasma samples. Briefly, a 2×10^{10} vector genome per milliliter solution of AAV9 capsids in 1 mM carbonate buffer were coated into a 96-well titer plate and incubated overnight at 4°C. The next day, the plate was washed and blocked with a 5% nonfat milk solution in PBST. Serum samples were diluted on range from 1:20 to 1:20,800 and incubated at room temperature for 2 h. Wells were then washed with PBST and incubated at room temperature for 1 h with a horseradish peroxidase-conjugated, donkey anti-sheep IgG (Abcam, Cambridge, UK) or rabbit anti-sheep IgM secondary antibody (Abcam). The wells were washed with again in PBST and then developed with 3,3′,5,5′-tetramethylbenzidine. The reaction was stopped by the addition of hydrochloric acid and the absorbance (optical density [O.D.]) was read at 450 nm on a plate reader. For both IgG and IgM, the titer was estimated as the last dilution with an O.D. reading 4-fold over the background O.D.

ELISA detection of anti-GFP antibodies

The ELISA for detecting anti-GFP antibodies was similar to the ELISA performed for the anti-AAV9 antibodies. The main difference was coating the assay plate with 100 μL GFP coating solution at a concentration of 0.5 mg/mL using Recombinant Victoria GFP protein (1 mg/mL) from Abcam.

Immunofluorescence

Tissues were fixed in 4% PFA at 4°C overnight, then washed in PBS and placed in 30% sucrose at 4°C for 48 h, after which they were embedded in OCT and frozen. We mounted 10- to 12-μm sections onto gelatin-coated slides and kept frozen at −80°C until staining was performed. Prior to staining, sections were dried, washed, and permeabilized with a 0.01% Triton solution for 20 min and blocked with 5% BSA for 1 h. The primary antibodies used were: GFP (dilution: 1:100-1:200; supplier: Thermo Fisher Scientific [Waltham, MA, USA]; Catalog #: G10362; Clone #: N/S; Lot #:2306774), NeuN (dilution: 1:200; supplier: Sigma-Aldrich [St. Louis, MO, USA]; Catalog #: MAB377A5; Clone #: A60; Lot #: 4015615), DDX4 (dilution: 1:200; supplier: Abcam, Catalog #: AB180462; Clone #: 27591; Lot #: GR3388842-3), HNF4a (dilution: 1:200; supplier: Invitrogen [Waltham, MA, USA]; Catalog #: MA1199; Clone #: K9218; Lot #: XG3618471), PAX7 (dilution: 1:100; supplier: Abcam; Catalog #: AB218472; Clone #:1187; Lot #: GR3452548-1), $CD45^+$ (dilution: 1:100; supplier: Bio-Rad; Catalog #: MCA2220GA; Clone #: 1.11.32; Lot #: 161823), $CD34^+$ (dilution: 1:100; supplier: BioLegend [San Diego, CA, USA]; Catalog #: 343608; Clone #: 561; Lot #: n/a), and laminin (dilution: 1:200; supplier: Thermo Fisher Scientific; Catalog #: MA106821; Clone #: N/S; Lot #: XI3696994 and XL3788692). The secondary antibodies used were goat anti-rabbit IgG AF488 (Supplier: Thermo Fisher Scientific; Catalog #: A11034; Clone #: N/S; Lot #: 2380031), donkey anti-mouse IgG AF555 (Supplier: Thermo Fisher Scientific; Catalog #: A31570; Clone #: N/S; Lot #:,2387458), and goat anti-rat IgG AF (Supplier: Abcam; Catalog #: AB150167; Clone #: n/s; Lot GR3429465-1) at a dilution equivalent to that of the corresponding primary antibody. After secondary antibody incubation, slides were mounted with mounting solution Fluoromount-G with DAPI (Invitrogen) and then cover-slipped. Images at 20× magnification were obtained on an Echo Revolve RVL2-K microscope and at 63× magnification on a Leica Microsystems (Wetzlar, Germany) Stellaris 5 microscope.

Immunohistochemical staining of DRGs

Slides were sectioned onto gelatine-coated slides at 20 mm. Slides were washed and then permeabilized and blocked with 3% BSA and 5% NGS in 0.03% Triton X-100 PBS for 1 h at room temperature. Primary antibody incubation was done overnight at 4°C with: GFP (dilution: 1:500; supplier: Thermo Fisher Scientific; Catalog #: A-11122; Clone #: N/S; Lot #:2339829) and Tuj1 (dilution: 1:1,000; supplier: Biolegend; Catalog #: 801202; Clone #TUJ1; Lot #: B199846). Secondary antibody incubation was done for 1 h at 4°C with goat anti-rabbit IgG AF488 (dilution: 1:1,000; supplier: Thermo Fisher Scientific; Catalog #: A11034; Clone #: N/S; Lot #: 2380031 and 1885241) and goat anti-mouse IgG555 (dilution: 1:1,000; supplier: Thermo Fisher Scientific; Catalog #: A21137; Clone #: N/S; Lot #: 2231667). Primary and secondary antibodies were diluted in the same blocking buffer to reduce background. Slides were then mounted with prolong-gold anti-fade reagent and cover slipped. Images at 63× were taken on a Zeiss (Jena, Germany) Axiovision Microscope.

For quantification of immunohistochemistry, three images per animal were taken at 10× magnification and saved in a .tif format. Images were deidentified to allow for blind interpretation of results and comparison between groups. For skeletal muscle samples, ImageJ was used to quantify GFP^+ cells, while individual muscular cells (identified by laminin staining) were counted manually. Transduction rates were averaged from the replicates of each animal.

DRG toxicity analysis

Toxicity analysis was done on C2, T3, L1, and L5 DRGs, which were fixed in formalin and embedded in paraffin to later be stained with toluidine blue. Blind analysis of slides was performed by a neuropathologist (C.C.) for chromatolysis, axonal loss, axonal degeneration, crush and traction artifacts, and regenerating clusters.

Laboratory testing of maternal and fetal blood

Maternal blood was obtained before *in utero* injection, at 1 day, 1 week, 3 weeks, and, for term harvests, 9 weeks after injection. Fetal blood was obtained at the time of harvest. All blood was analyzed by the University of California Davis Comparative Pathology Laboratory (CPL). Lab values from samples that were hemolyzed (as indicated by CPL) were excluded from analysis (three fetal and three maternal samples).

Pathology

Aliquots of tissues were fixed in formalin and embedded in paraffin to later be stained with hematoxylin and eosin. Formalin-fixed paraffin-embedded tissues were sectioned and stained with hematoxylin and eosin to assess histological changes and any disruption in cellular architecture. Liver samples were graded based on the presence

of pigment accumulation and bile canalicular stasis with the following scoring system: 0 (not present), 1 (pigment only), and 2 (pigment and bile canalicular stasis). Kidney samples were graded based on the presence of pigment accumulation and tubular epithelial necrosis with the following scoring system: 0 (not present), 1 (pigment), and 2 (tubular epithelial necrosis). Grading was done in a blinded fashion by an experienced veterinary pathologist (D.I.L.). Composite lesion scores (sum of the scores for liver and kidney findings) were calculated for each group.

Integration analysis

Integration analysis was performed by ProtaGene (www.protagene.com). Standard S-EPTS/LM-PCR and deep sequencing were performed to identify adeno-associated viral vector flanking genomic sequences in three ovary (1967A, 1974B, and 2134B) and three testes (1974C, 2135A, and 2135B) samples transduced with the vector. Briefly, 1,500 ng genomic DNA per sample were sheared to a median length of 500 bp, purified, and split equally into triplicates. Primer extension was performed using a bovine growth hormone polyadenylation signal-specific biotinylated primer (AMT1bio). The extension product was again purified, followed by magnetic capture of the biotinylated DNA. The captured DNA was ligated to linker cassettes, including a molecular barcode. The ligation product was amplified in a first exponential PCR using biotinylated vector and linker cassette-specific primers. Biotinylated PCR products were magnetically captured, washed, and one-half of this eluate served as template for amplification in a second exponential PCR step allowing deep sequencing by MiSeq technology (Illumina, San Diego, CA, USA) after purification. Preparation for deep sequencing has been previously described.[71,72]

After identification of ISs through S-EPTS/LM-PCR,[73] they were analyzed using the GENE-IS tool suite.[74] Raw data were filtered and only sequences showing complete identity in molecular barcodes, linker cassette barcode, and sequencing barcode were further processed. The detected ISs were clustered based on their determined location (position on genome of reference) for each replicate individually using a ±10 bp range. Then, a second clustering was performed on the sample level to group datasets of the corresponding replicates using a ±5 bp range. After clustering, sequences matching the vector sequence with a defined coverage and identity are removed as being assay artifacts due to amplification of non-integrated or concatenated vector. Then, IS position data combined from all samples were plotted to display chromosomal distribution, integration within gene coding regions and vicinity (10 kb upstream and downstream) integration relative to transcription start sties and relative positions within gene coding.

Common IS analysis

A systems biology approach was used to dissect biologically relevant IS clusters, as previously described,[75] to allow the identification of positional IS accumulations that are statistically unlikely to occur by chance.[76,77] Analysis of IS and proximity to cancer-associated genes was performed by first obtaining cancer-related genes from the Catalog of Somatic Mutations in Cancer Cancer Gene Census.[78] For this study, a lift-over from the sheep genome (oviAri4) to the human genome (hg38) was required to perform the analysis (UCSC Assembly). Cancer gene annotations (chromosome, gene start, gene end, strand, gene name, transcript count, and transcription start site) were obtained from the Ensembl human genes. While adverse events in gene therapy trials have been attributed to integration within 40 kB,[39–44] since other studies describe deregulation of genes within 300 kB,[79–81] an arbitrary window of 100 kB was investigated by ProtaGene.

STATISTICAL ANALYSIS

Results were graphed and analyzed using statistical software GraphPad Prism version 9.5.1 (GraphPad Software, La Jolla, CA, USA). All measurements were taken from distinct animal samples and no repeated measurements were taken. Parametric data were analyzed via two-tailed paired (for maternal laboratory values only) and unpaired t tests, and one-way ANOVA test with Tukey's multiple comparison test. Non-parametric data were analyzed via Wilcoxon signed rank test (for antibody titers and histological grading of liver and kidney), the Mann-Whitney test (for quantification of $GFP^{+}laminin^{+}$ cells), and the Kruskal-Wallis test (for histological grading of DRG). Statistical support was provided by the Department of Surgery Biostatistics Core.

DATA AND CODE AVAILABILITY

All data supporting the findings of this study are either available within the paper and its Supplementary Information or can be provided by contacting the corresponding author.

SUPPLEMENTAL INFORMATION

Supplemental information can be found online at https://doi.org/10.1016/j.omtm.2024.101263.

ACKNOWLEDGMENTS

This work was funded by a sponsored research agreement from Novartis (T.C.M.), NIH grant R35NS122306 (C.J.S.), and funds from the UCSF Center for Maternal-Fetal Precision Medicine (CMFPM). We thank Jasmine Wu, Pervinder Kaur Choksi, Shalini Namuduri, Annie Cao, Tim Rath, Richard Gabriel, Iris Anne Valent, and Jordan Jackson for technical assistance. We thank members of the MacKenzie Lab, the UCSF CMFPM, and Alta Charo for helpful discussions.

AUTHOR CONTRIBUTIONS

T.C.M. conceptualized the project and aims with input from C.J.S. and N.G. T.C.M., M.S., A.V., C.P., M.C., A.H., N.G., and B.B. performed *in utero* surgeries and tissue harvesting. G.G., S.P., T.D.R., and F.O. performed ddPCR and ELISA assays. T.C.M., B.B., A.V., M.C., L.K., C.J.S., D.J.L., and D.I.L. designed, performed, and/or analyzed histopathological analysis of various organs. T.C.M., B.B, and A.V. prepared figures and wrote the manuscript with input from the authors.

DECLARATION OF INTERESTS

G.G., S.P., T.D.R., and F.O. are employees and stockholders of Novartis. C.J.S. receives grant support from Roche Ltd., Biogen, and Actio

Bio and has served as a paid advisor, consultant, and/or speaker to Biogen, Roche/Genentech, and Novartis; these arrangements have been reviewed and approved by the Johns Hopkins University in accordance with its conflict-of-interest policies. T.C.M. receives grant funding from Novartis, BioMarin, and Biogen and is on the SAB of Acrigen; these arrangements have been reviewed and approved by UCSF in accordance with its conflict of interest policies.

REFERENCES

1. Herzeg, A., Almeida-Porada, G., Charo, R.A., David, A.L., Gonzalez-Velez, J., Gupta, N., Lapteva, L., Lianoglou, B., Peranteau, W., Porada, C., et al. (2022). Prenatal Somatic Cell Gene Therapies: Charting a Path Toward Clinical Applications (Proceedings of the CERSI-FDA Meeting). J. Clin. Pharmacol. *62*, S36–S52. https://doi.org/10.1002/jcph.2127.
2. Almeida-Porada, G., Atala, A., and Porada, C.D. (2016). In utero stem cell transplantation and gene therapy: rationale, history, and recent advances toward clinical application. Mol. Ther. Methods Clin. Dev. *5*, 16020. https://doi.org/10.1038/mtm.2016.20.
3. Schwab, M.E., and MacKenzie, T.C. (2021). Prenatal Gene Therapy. Clin. Obstet. Gynecol. *64*, 876–885. https://doi.org/10.1097/GRF.0000000000000655.
4. Shen, J.S., Meng, X.L., Maeda, H., Ohashi, T., and Eto, Y. (2004). Widespread gene transduction to the central nervous system by adenovirus in utero: implication for prenatal gene therapy to brain involvement of lysosomal storage disease. J. Gene Med. *6*, 1206–1215. https://doi.org/10.1002/jgm.630.
5. Chan, J.K.Y., Gil-Farina, I., Johana, N., Rosales, C., Tan, Y.W., Ceiler, J., McIntosh, J., Ogden, B., Waddington, S.N., Schmidt, M., et al. (2019). Therapeutic expression of human clotting factors IX and X following adeno-associated viral vector-mediated intrauterine gene transfer in early-gestation fetal macaques. FASEB J. *33*, 3954–3967. https://doi.org/10.1096/fj.201801391R.
6. Mattar, C.N.Z., Gil-Farina, I., Rosales, C., Johana, N., Tan, Y.Y.W., McIntosh, J., Kaeppel, C., Waddington, S.N., Biswas, A., Choolani, M., et al. (2017). In Utero Transfer of Adeno-Associated Viral Vectors Produces Long-Term Factor IX Levels in a Cynomolgus Macaque Model. Mol. Ther. *25*, 1843–1853. https://doi.org/10.1016/j.ymthe.2017.04.003.
7. Palanki, R., Peranteau, W.H., and Mitchell, M.J. (2021). Delivery technologies for in utero gene therapy. Adv. Drug Deliv. Rev. *169*, 51–62. https://doi.org/10.1016/j.addr.2020.11.002.
8. Cohen, J.L., Chakraborty, P., Fung-Kee-Fung, K., Schwab, M.E., Bali, D., Young, S.P., Gelb, M.H., Khaledi, H., DiBattista, A., Smallshaw, S., et al. (2022). In Utero Enzyme-Replacement Therapy for Infantile-Onset Pompe's Disease. N. Engl. J. Med. *387*, 2150–2158. https://doi.org/10.1056/NEJMoa2200587.
9. Committee Opinion No. 691: Carrier Screening for Genetic Conditions (2017). Obstet. Gynecol. *129*, e41–e55. https://doi.org/10.1097/AOG.0000000000001952.
10. Kong, L., Valdivia, D.O., Simon, C.M., Hassinan, C.W., Delestrée, N., Ramos, D.M., Park, J.H., Pilato, C.M., Xu, X., Crowder, M., et al. (2021). Impaired prenatal motor axon development necessitates early therapeutic intervention in severe SMA. Sci. Transl. Med. *13*, eabb6871. https://doi.org/10.1126/scitranslmed.abb6871.
11. Darras, B.T., Crawford, T.O., Finkel, R.S., Mercuri, E., De Vivo, D.C., Oskoui, M., Tizzano, E.F., Ryan, M.M., Muntoni, F., Zhao, G., et al. (2019). Neurofilament as a potential biomarker for spinal muscular atrophy. Ann. Clin. Transl. Neurol. *6*, 932–944. https://doi.org/10.1002/acn3.779.
12. Foust, K.D., Nurre, E., Montgomery, C.L., Hernandez, A., Chan, C.M., and Kaspar, B.K. (2009). Intravascular AAV9 preferentially targets neonatal neurons and adult astrocytes. Nat. Biotechnol. *27*, 59–65. https://doi.org/10.1038/nbt.1515.
13. Mattar, C.N., Waddington, S.N., Biswas, A., Johana, N., Ng, X.W., Fisk, A.S., Fisk, N.M., Tan, L.G., Rahim, A.A., Buckley, S.M.K., et al. (2013). Systemic delivery of scAAV9 in fetal macaques facilitates neuronal transduction of the central and peripheral nervous systems. Gene Ther. *20*, 69–83. https://doi.org/10.1038/gt.2011.216.
14. Zaiss, A.K., and Muruve, D.A. (2005). Immune responses to adeno-associated virus vectors. Curr. Gene Ther. *5*, 323–331. https://doi.org/10.2174/1566523054065039.
15. Penaud-Budloo, M., Le Guiner, C., Nowrouzi, A., Toromanoff, A., Chérel, Y., Chenuaud, P., Schmidt, M., von Kalle, C., Rolling, F., Moullier, P., and Snyder, R.O. (2008). Adeno-associated virus vector genomes persist as episomal chromatin in primate muscle. J. Virol. *82*, 7875–7885. https://doi.org/10.1128/JVI.00649-08.
16. Schnepp, B.C., Clark, K.R., Klemanski, D.L., Pacak, C.A., and Johnson, P.R. (2003). Genetic fate of recombinant adeno-associated virus vector genomes in muscle. J. Virol. *77*, 3495–3504. https://doi.org/10.1128/jvi.77.6.3495-3504.2003.
17. Schnepp, B.C., Jensen, R.L., Chen, C.L., Johnson, P.R., and Clark, K.R. (2005). Characterization of adeno-associated virus genomes isolated from human tissues. J. Virol. *79*, 14793–14803. https://doi.org/10.1128/JVI.79.23.14793-14803.2005.
18. Zincarelli, C., Soltys, S., Rengo, G., and Rabinowitz, J.E. (2008). Analysis of AAV serotypes 1-9 mediated gene expression and tropism in mice after systemic injection. Mol. Ther. *16*, 1073–1080. https://doi.org/10.1038/mt.2008.76.
19. Mendell, J.R., Al-Zaidy, S., Shell, R., Arnold, W.D., Rodino-Klapac, L.R., Prior, T.W., Lowes, L., Alfano, L., Berry, K., Church, K., et al. (2017). Single-Dose Gene-Replacement Therapy for Spinal Muscular Atrophy. N. Engl. J. Med. *377*, 1713–1722. https://doi.org/10.1056/NEJMoa1706198.
20. Mendell, J.R., Sahenk, Z., Lehman, K., Nease, C., Lowes, L.P., Miller, N.F., Iammarino, M.A., Alfano, L.N., Nicholl, A., Al-Zaidy, S., et al. (2020). Assessment of Systemic Delivery of rAAVrh74.MHCK7.micro-dystrophin in Children With Duchenne Muscular Dystrophy: A Nonrandomized Controlled Trial. JAMA Neurol. *77*, 1122–1131. https://doi.org/10.1001/jamaneurol.2020.1484.
21. Sabatino, D.E., Mackenzie, T.C., Peranteau, W., Edmonson, S., Campagnoli, C., Liu, Y.L., Flake, A.W., and High, K.A. (2007). Persistent expression of hF.IX After tolerance induction by in utero or neonatal administration of AAV-1-F.IX in hemophilia B mice. Mol. Ther. *15*, 1677–1685. https://doi.org/10.1038/sj.mt.6300219.
22. Waddington, S.N., Nivsarkar, M.S., Mistry, A.R., Buckley, S.M.K., Kemball-Cook, G., Mosley, K.L., Mitrophanous, K., Radcliffe, P., Holder, M.V., Brittan, M., et al. (2004). Permanent phenotypic correction of hemophilia B in immunocompetent mice by prenatal gene therapy. Blood *104*, 2714–2721. https://doi.org/10.1182/blood-2004-02-0627.
23. Rashnonejad, A., Amini Chermahini, G., Gündüz, C., Onay, H., Aykut, A., Durmaz, B., Baka, M., Su, Q., Gao, G., and Özkınay, F. (2019). Fetal Gene Therapy Using a Single Injection of Recombinant AAV9 Rescued SMA Phenotype in Mice. Mol. Ther. *27*, 2123–2133. https://doi.org/10.1016/j.ymthe.2019.08.017.
24. Massaro, G., Mattar, C.N.Z., Wong, A.M.S., Sirka, E., Buckley, S.M.K., Herbert, B.R., Karlsson, S., Perocheau, D.P., Burke, D., Heales, S., et al. (2018). Fetal gene therapy for neurodegenerative disease of infants. Nat. Med. *24*, 1317–1323. https://doi.org/10.1038/s41591-018-0106-7.
25. Wolter, J.M., Mao, H., Fragola, G., Simon, J.M., Krantz, J.L., Bazick, H.O., Oztemiz, B., Stein, J.L., and Zylka, M.J. (2020). Cas9 gene therapy for Angelman syndrome traps Ube3a-ATS long non-coding RNA. Nature *587*, 281–284. https://doi.org/10.1038/s41586-020-2835-2.
26. Bose, S.K., White, B.M., Kashyap, M.V., Dave, A., De Bie, F.R., Li, H., Singh, K., Menon, P., Wang, T., Teerdhala, S., et al. (2021). In utero adenine base editing corrects multi-organ pathology in a lethal lysosomal storage disease. Nat. Commun. *12*, 4291. https://doi.org/10.1038/s41467-021-24443-8.
27. Mukherjee, P., Roy, S., Ghosh, D., and Nandi, S.K. (2022). Role of animal models in biomedical research: a review. Lab. Anim. Res. *38*, 18. https://doi.org/10.1186/s42826-022-00128-1.
28. Scheerlinck, J.P.Y., Snibson, K.J., Bowles, V.M., and Sutton, P. (2008). Biomedical applications of sheep models: from asthma to vaccines. Trends Biotechnol. *26*, 259–266. https://doi.org/10.1016/j.tibtech.2008.02.002.
29. Kabagambe, S.K., Lee, C.J., Goodman, L.F., Chen, Y.J., Vanover, M.A., and Farmer, D.L. (2018). Lessons from the Barn to the Operating Suite: A Comprehensive Review of Animal Models for Fetal Surgery. Annu. Rev. Anim. Biosci. *6*, 99–119. https://doi.org/10.1146/annurev-animal-030117-014637.
30. Thomsen, G., Burghes, A.H.M., Hsieh, C., Do, J., Chu, B.T.T., Perry, S., Barkho, B., Kaufmann, P., Sproule, D.M., Feltner, D.E., et al. (2021). Biodistribution of onasemnogene abeparvovec DNA, mRNA and SMN protein in human tissue. Nat. Med. *27*, 1701–1711. https://doi.org/10.1038/s41591-021-01483-7.
31. Bevan, A.K., Duque, S., Foust, K.D., Morales, P.R., Braun, L., Schmelzer, L., Chan, C.M., McCrate, M., Chicoine, L.G., Coley, B.D., et al. (2011). Systemic gene delivery

in large species for targeting spinal cord, brain, and peripheral tissues for pediatric disorders. Mol. Ther. *19*, 1971–1980. https://doi.org/10.1038/mt.2011.157.

32. Hinderer, C., Katz, N., Buza, E.L., Dyer, C., Goode, T., Bell, P., Richman, L.K., and Wilson, J.M. (2018). Severe Toxicity in Nonhuman Primates and Piglets Following High-Dose Intravenous Administration of an Adeno-Associated Virus Vector Expressing Human SMN. Hum. Gene Ther. *29*, 285–298. https://doi.org/10.1089/hum.2018.015.

33. Hordeaux, J., Buza, E.L., Dyer, C., Goode, T., Mitchell, T.W., Richman, L., Denton, N., Hinderer, C., Katz, N., Schmid, R., et al. (2020). Adeno-Associated Virus-Induced Dorsal Root Ganglion Pathology. Hum. Gene Ther. *31*, 808–818. https://doi.org/10.1089/hum.2020.167.

34. Hordeaux, J., Hinderer, C., Goode, T., Buza, E.L., Bell, P., Calcedo, R., Richman, L.K., and Wilson, J.M. (2018). Toxicology Study of Intra-Cisterna Magna Adeno-Associated Virus 9 Expressing Iduronate-2-Sulfatase in Rhesus Macaques. Mol. Ther. Methods Clin. Dev. *10*, 68–78. https://doi.org/10.1016/j.omtm.2018.06.004.

35. Hordeaux, J., Hinderer, C., Goode, T., Katz, N., Buza, E.L., Bell, P., Calcedo, R., Richman, L.K., and Wilson, J.M. (2018). Toxicology Study of Intra-Cisterna Magna Adeno-Associated Virus 9 Expressing Human Alpha-L-Iduronidase in Rhesus Macaques. Mol. Ther. Methods Clin. Dev. *10*, 79–88. https://doi.org/10.1016/j.omtm.2018.06.003.

36. Rich, K.A., Wier, C.G., Russo, J., Kong, L., Heilman, P.L., Reynolds, A., Knapp, A., Pino, M.G., Keckley, E., Mattox, L., et al. (2022). Premature delivery in the domestic sow in response to in utero delivery of AAV9 to fetal piglets. Gene Ther. *29*, 513–519. https://doi.org/10.1038/s41434-021-00305-2.

37. Castrillon, D.H., Quade, B.J., Wang, T.Y., Quigley, C., and Crum, C.P. (2000). The human VASA gene is specifically expressed in the germ cell lineage. Proc. Natl. Acad. Sci. USA *97*, 9585–9590. https://doi.org/10.1073/pnas.160274797.

38. Abbas, A.K., Lichtman, A.H., Pillai, S., Baker, D.L., and Baker, A. (2018). Cellular and Molecular Immunology, Ninth edition (Elsevier).

39. Deichmann, A., Hacein-Bey-Abina, S., Schmidt, M., Garrigue, A., Brugman, M.H., Hu, J., Glimm, H., Gyapay, G., Prum, B., Fraser, C.C., et al. (2007). Vector integration is nonrandom and clustered and influences the fate of lymphopoiesis in SCID-X1 gene therapy. J. Clin. Invest. *117*, 2225–2232. https://doi.org/10.1172/JCI31659.

40. Hacein-Bey-Abina, S., Garrigue, A., Wang, G.P., Soulier, J., Lim, A., Morillon, E., Clappier, E., Caccavelli, L., Delabesse, E., Beldjord, K., et al. (2008). Insertional oncogenesis in 4 patients after retrovirus-mediated gene therapy of SCID-X1. J. Clin. Invest. *118*, 3132–3142. https://doi.org/10.1172/JCI35700.

41. Hacein-Bey-Abina, S., von Kalle, C., Schmidt, M., Le Deist, F., Wulffraat, N., McIntyre, E., Radford, I., Villeval, J.L., Fraser, C.C., Cavazzana-Calvo, M., and Fischer, A. (2003). A serious adverse event after successful gene therapy for X-linked severe combined immunodeficiency. N. Engl. J. Med. *348*, 255–256. https://doi.org/10.1056/NEJM200301163480314.

42. Hacein-Bey-Abina, S., Von Kalle, C., Schmidt, M., McCormack, M.P., Wulffraat, N., Leboulch, P., Lim, A., Osborne, C.S., Pawliuk, R., Morillon, E., et al. (2003). LMO2-associated clonal T cell proliferation in two patients after gene therapy for SCID-X1. Science *302*, 415–419. https://doi.org/10.1126/science.1088547.

43. Howe, S.J., Mansour, M.R., Schwarzwaelder, K., Bartholomae, C., Hubank, M., Kempski, H., Brugman, M.H., Pike-Overzet, K., Chatters, S.J., de Ridder, D., et al. (2008). Insertional mutagenesis combined with acquired somatic mutations causes leukemogenesis following gene therapy of SCID-X1 patients. J. Clin. Invest. *118*, 3143–3150. https://doi.org/10.1172/JCI35798.

44. Ott, M.G., Schmidt, M., Schwarzwaelder, K., Stein, S., Siler, U., Koehl, U., Glimm, H., Kühlcke, K., Schilz, A., Kunkel, H., et al. (2006). Correction of X-linked chronic granulomatous disease by gene therapy, augmented by insertional activation of MDS1-EVI1, PRDM16 or SETBP1. Nat. Med. *12*, 401–409. https://doi.org/10.1038/nm1393.

45. Mahlangu, J., Kaczmarek, R., von Drygalski, A., Shapiro, S., Chou, S.C., Ozelo, M.C., Kenet, G., Peyvandi, F., Wang, M., Madan, B., et al. (2023). Two-Year Outcomes of Valoctocogene Roxaparvovec Therapy for Hemophilia A. N. Engl. J. Med. *388*, 694–705. https://doi.org/10.1056/NEJMoa2211075.

46. Guillou, J., de Pellegars, A., Porcheret, F., Frémeaux-Bacchi, V., Allain-Launay, E., Debord, C., Denis, M., Péréon, Y., Barnérias, C., Desguerre, I., et al. (2022). Fatal thrombotic microangiopathy case following adeno-associated viral SMN gene therapy. Blood Adv. *6*, 4266–4270. https://doi.org/10.1182/bloodadvances.2021006419.

47. Chand, D., Mohr, F., McMillan, H., Tukov, F.F., Montgomery, K., Kleyn, A., Sun, R., Tauscher-Wisniewski, S., Kaufmann, P., and Kullak-Ublick, G. (2021). Hepatotoxicity following administration of onasemnogene abeparvovec (AVXS-101) for the treatment of spinal muscular atrophy. J. Hepatol. *74*, 560–566. https://doi.org/10.1016/j.jhep.2020.11.001.

48. Wilson, J.M., and Flotte, T.R. (2020). Moving Forward After Two Deaths in a Gene Therapy Trial of Myotubular Myopathy. Hum. Gene Ther. *31*, 695–696. https://doi.org/10.1089/hum.2020.182.

49. High-dose AAV gene therapy deaths (2020). Nat. Biotechnol. *38*, 910. https://doi.org/10.1038/s41587-020-0642-9.

50. FDA (2021). Food and Drug Administration (FDA) Cellular, Tissue, and Gene Therapies Advisory Committee (CTGTAC) Meeting #70; Toxicity Risks of Adeno-Associated Virus (AAV) Vectors for Gene Therapy.

51. Davey, M.G., Riley, J.S., Andrews, A., Tyminski, A., Limberis, M., Pogoriler, J.E., Partridge, E., Olive, A., Hedrick, H.L., Flake, A.W., and Peranteau, W.H. (2017). Induction of Immune Tolerance to Foreign Protein via Adeno-Associated Viral Vector Gene Transfer in Mid-Gestation Fetal Sheep. PLoS One *12*, e0171132. https://doi.org/10.1371/journal.pone.0171132.

52. David, A.L., McIntosh, J., Peebles, D.M., Cook, T., Waddington, S., Weisz, B., Wigley, V., Abi-Nader, K., Boyd, M., Davidoff, A.M., and Nathwani, A.C. (2011). Recombinant adeno-associated virus-mediated in utero gene transfer gives therapeutic transgene expression in the sheep. Hum. Gene Ther. *22*, 419–426. https://doi.org/10.1089/hum.2010.007.

53. Gardner, D.S., Buttery, P.J., Daniel, Z., and Symonds, M.E. (2007). Factors affecting birth weight in sheep: maternal environment. Reproduction *133*, 297–307. https://doi.org/10.1530/REP-06-0042.

54. Freetly, H.C., and Leymaster, K.A. (2004). Relationship between litter birth weight and litter size in six breeds of sheep. J. Anim. Sci. *82*, 612–618. https://doi.org/10.2527/2004.822612x.

55. Ansari, A.M., Ahmed, A.K., Matsangos, A.E., Lay, F., Born, L.J., Marti, G., Harmon, J.W., and Sun, Z. (2016). Cellular GFP Toxicity and Immunogenicity: Potential Confounders in in Vivo Cell Tracking Experiments. Stem Cell Rev. Rep. *12*, 553–559. https://doi.org/10.1007/s12015-016-9670-8.

56. Barry, J.S., and Anthony, R.V. (2008). The pregnant sheep as a model for human pregnancy. Theriogenology *69*, 55–67. https://doi.org/10.1016/j.theriogenology.2007.09.021.

57. Bonnemann, C.G., Belluscio, B.A., Braun, S., Morris, C., Singh, T., and Muntoni, F. (2023). Dystrophin Immunity after Gene Therapy for Duchenne's Muscular Dystrophy. N. Engl. J. Med. *388*, 2294–2296. https://doi.org/10.1056/NEJMc2212912.

58. Meseck, E.K., Guibinga, G., Wang, S., McElroy, C., Hudry, E., and Mansfield, K. (2022). Intrathecal sc-AAV9-CB-GFP: Systemic Distribution Predominates Following Single-Dose Administration in Cynomolgus Macaques. Toxicol. Pathol. *50*, 415–431. https://doi.org/10.1177/01926233221101309.

59. Logan, G.J., Mietzsch, M., Khandekar, N., D'Silva, A., Anderson, D., Mandwie, M., Hsi, J., Nelson, A.R., Chipman, P., Jackson, J., et al. (2023). Structural and functional characterization of capsid binding by anti-AAV9 monoclonal antibodies from infants after SMA gene therapy. Mol. Ther. *31*, 1979–1993. https://doi.org/10.1016/j.ymthe.2023.03.032.

60. McLaren, A. (1984). Meiosis and differentiation of mouse germ cells. Symp. Soc. Exp. Biol. *38*, 7–23.

61. Hilscher, W. (1974). [Kinetics of prespermatogenesis and spermatogenesis]. Verhandlungen Anat. Ges. *68*, 39–62.

62. Nguyen, G.N., Everett, J.K., Kafle, S., Roche, A.M., Raymond, H.E., Leiby, J., Wood, C., Assenmacher, C.A., Merricks, E.P., Long, C.T., et al. (2021). A long-term study of AAV gene therapy in dogs with hemophilia A identifies clonal expansions of transduced liver cells. Nat. Biotechnol. *39*, 47–55. https://doi.org/10.1038/s41587-020-0741-7.

63. Donsante, A., Vogler, C., Muzyczka, N., Crawford, J.M., Barker, J., Flotte, T., Campbell-Thompson, M., Daly, T., and Sands, M.S. (2001). Observed incidence of tumorigenesis in long-term rodent studies of rAAV vectors. Gene Ther. *8*, 1343–1346. https://doi.org/10.1038/sj.gt.3301541.

64. Mastroianni, L., and Coutifaris, C. (1990). The FIGO Manual of Human Reproduction. Vol 1. Reproductive Physiology (Park Ridge: Parthenon Publishing).

65. Gentner, B., Visigalli, I., Hiramatsu, H., Lechman, E., Ungari, S., Giustacchini, A., Schira, G., Amendola, M., Quattrini, A., Martino, S., et al. (2010). Identification of hematopoietic stem cell-specific miRNAs enables gene therapy of globoid cell leukodystrophy. Sci. Transl. Med. *2*, 58ra84. https://doi.org/10.1126/scitranslmed.3001522.

66. Schwab, M.E., Shao, S., Zhang, L., Lianoglou, B., Belter, L., Jarecki, J., Schroth, M., Sumner, C.J., and MacKenzie, T. (2022). Investigating attitudes toward prenatal diagnosis and fetal therapy for spinal muscular atrophy. Prenat. Diagn. *42*, 1409–1419. https://doi.org/10.1002/pd.6228.

67. Strauss, K.A., Farrar, M.A., Muntoni, F., Saito, K., Mendell, J.R., Servais, L., McMillan, H.J., Finkel, R.S., Swoboda, K.J., Kwon, J.M., et al. (2022). Onasemnogene abeparvovec for presymptomatic infants with two copies of SMN2 at risk for spinal muscular atrophy type 1: the Phase III SPR1NT trial. Nat. Med. *28*, 1381–1389. https://doi.org/10.1038/s41591-022-01866-4.

68. Bell, A.W., Kennaugh, J.M., Battaglia, F.C., Makowski, E.L., and Meschia, G. (1986). Metabolic and circulatory studies of fetal lamb at midgestation. Am. J. Physiol. *250*, E538–E544. https://doi.org/10.1152/ajpendo.1986.250.5.E538.

69. Molina, R.D., Meschia, G., and Wilkening, R.B. (1990). Uterine blood flow, oxygen and glucose uptakes at mid-gestation in the sheep. Proc. Soc. Exp. Biol. Med. *195*, 379–385. https://doi.org/10.3181/00379727-195-43158aa.

70. Meyer, A., Pellaux, R., Potot, S., Becker, K., Hohmann, H.P., Panke, S., and Held, M. (2015). Optimization of a whole-cell biocatalyst by employing genetically encoded product sensors inside nanolitre reactors. Nat. Chem. *7*, 673–678. https://doi.org/10.1038/nchem.2301.

71. Paruzynski, A., Arens, A., Gabriel, R., Bartholomae, C.C., Scholz, S., Wang, W., Wolf, S., Glimm, H., Schmidt, M., and von Kalle, C. (2010). Genome-wide high-throughput integrome analyses by nrLAM-PCR and next-generation sequencing. Nat. Protoc. *5*, 1379–1395. https://doi.org/10.1038/nprot.2010.87.

72. Gabriel, R., Eckenberg, R., Paruzynski, A., Bartholomae, C.C., Nowrouzi, A., Arens, A., Howe, S.J., Recchia, A., Cattoglio, C., Wang, W., et al. (2009). Comprehensive genomic access to vector integration in clinical gene therapy. Nat. Med. *15*, 1431–1436. https://doi.org/10.1038/nm.2057.

73. Schmidt, M., Hoffmann, G., Wissler, M., Lemke, N., Müssig, A., Glimm, H., Williams, D.A., Ragg, S., Hesemann, C.U., and von Kalle, C. (2001). Detection and direct genomic sequencing of multiple rare unknown flanking DNA in highly complex samples. Hum. Gene Ther. *12*, 743–749. https://doi.org/10.1089/104303401750148649.

74. Afzal, S., Wilkening, S., von Kalle, C., Schmidt, M., and Fronza, R. (2017). GENE-IS: Time-Efficient and Accurate Analysis of Viral Integration Events in Large-Scale Gene Therapy Data. Mol. Ther. Nucleic Acids *6*, 133–139. https://doi.org/10.1016/j.omtn.2016.12.001.

75. Fronza, R., Vasciaveo, A., Benso, A., and Schmidt, M. (2016). A Graph Based Framework to Model Virus Integration Sites. Comput. Struct. Biotechnol. J. *14*, 69–77. https://doi.org/10.1016/j.csbj.2015.10.006.

76. Abel, U., Deichmann, A., Nowrouzi, A., Gabriel, R., Bartholomae, C.C., Glimm, H., von Kalle, C., and Schmidt, M. (2011). Analyzing the number of common integration sites of viral vectors–new methods and computer programs. PLoS One *6*, e24247. https://doi.org/10.1371/journal.pone.0024247.

77. Shen, H., Suzuki, T., Munroe, D.J., Stewart, C., Rasmussen, L., Gilbert, D.J., Jenkins, N.A., and Copeland, N.G. (2003). Common sites of retroviral integration in mouse hematopoietic tumors identified by high-throughput, single nucleotide polymorphism-based mapping and bacterial artificial chromosome hybridization. J. Virol. *77*, 1584–1588. https://doi.org/10.1128/jvi.77.2.1584-1588.2003.

78. Alsulami, A.F., Torres, P.H.M., Moghul, I., Arif, S.M., Chaplin, A.K., Vedithi, S.C., and Blundell, T.L. (2021). COSMIC Cancer Gene Census 3D database: understanding the impacts of mutations on cancer targets. Briefings Bioinf. *22*, bbab220. https://doi.org/10.1093/bib/bbab220.

79. Recchia, A., Bonini, C., Magnani, Z., Urbinati, F., Sartori, D., Muraro, S., Tagliafico, E., Bondanza, A., Stanghellini, M.T.L., Bernardi, M., et al. (2006). Retroviral vector integration deregulates gene expression but has no consequence on the biology and function of transplanted T cells. Proc. Natl. Acad. Sci. USA *103*, 1457–1462. https://doi.org/10.1073/pnas.0507496103.

80. Hargrove, P.W., Kepes, S., Hanawa, H., Obenauer, J.C., Pei, D., Cheng, C., Gray, J.T., Neale, G., and Persons, D.A. (2008). Globin lentiviral vector insertions can perturb the expression of endogenous genes in beta-thalassemic hematopoietic cells. Mol. Ther. *16*, 525–533. https://doi.org/10.1038/sj.mt.6300394.

81. Melamed, A., Yaguchi, H., Miura, M., Witkover, A., Fitzgerald, T.W., Birney, E., and Bangham, C.R. (2018). The human leukemia virus HTLV-1 alters the structure and transcription of host chromatin in cis. Elife *7*, e36245. https://doi.org/10.7554/eLife.36245.